

On wave interaction and diffraction from the junction of two curved plates under unilateral fluid loading

By A. N. Norris¹, D. A. Rebinsky¹ and G. R. Wickham²†

¹Department of Mechanical and Aerospace Engineering, Rutgers University, Piscataway, NJ 08854-8058, USA ²Department of Mathematics and Statistics, Brunel University, Uxbridge, Middlesex UB8 3PH, UK

Received 17 May 1996; accepted 21 May 1997

Contents

1	Introduction	1421
	General theory	1423
3.	· · · · · · · · · · · · · · · · · · ·	1424
4.	The dispersion relation and reflection by a homogeneous plate	1427
1.	(a) Dispersion relation	1427
	(b) Reflection coefficients	1428
	(c) Shell waves	1429
5.	Formal solution of the diffraction problem	1430
•	(a) Incident and scattered fields	1430
	(b) General solution	1431
	(c) Displacement and stress solutions	1432
	(d) Diffraction coefficients	1432
	(e) Consequences of reciprocity	1434
	(f) Energy conservation	1434
6.	Satisfying the join conditions	1436
	(a) Alternative integral forms for w_0 and p_0	1436
	(b) Behaviour of w_0 and p_0 near the join	1438
	(c) Determination of $A(\xi)$	1439
7.	Limiting cases	1442
	(a) Identical plates: change in curvature	1442
	(b) One flat plate	1442
	(c) FPL*	1444
	(d) Two flat plates	1444
8.	Numerical results	1446
9.	Conclusions	1451
Αı	opendix A. Factorization of the dispersion functions	1454
•	(a) Preliminary results and definitions	1454
	(b) Analytic splitting	1455
	(c) Evaluating the residues	1456

(d) Number of physical roots	1458
(e) Various forms of K^+	1458
Appendix B. Expansion coefficients	1459
(a) Asymptotic forms for K^+	1459
(b) Expansions for \tilde{w}_0^{\pm} and \tilde{p}_0^{\pm}	1461
Appendix C. Meaning for the roots of $P^*(\xi) = 0$	1462
Appendix D. Two membranes	1463
(a) Light fluid-loading limit	1464
(b) Heavy fluid-loading approximation	1465

A general solution is developed which describes the acoustic and dynamic structural response generated at the junction of two curved plates subject to unilateral fluid loading. The plates are modelled by two-dimensional thin-shell theory, and the solution is found by applying the Wiener-Hopf technique to the dual integral equations for the unknown pressure on the plates. A simple method is presented for evaluating the Wiener-Hopf split functions in semi-analytic form. The general solution is found by expressing the pressure transform in terms of a polynomial function whose coefficients are determined by the conditions at the joint. Here we consider welded and clamped junctions, either of which requires four unknown coefficients to be determined. Several limiting cases are examined including the practically important ones where either one or both plates are flat. Various diffraction coefficients associated with the fluid-structure interaction are studied and numerical predictions are presented for the magnitudes of the diffracted acoustic and structural waves. Energy partition among the various wave types is also investigated. It is found that even the small curvature effects considered here can lead to significant coupling between flexural and longitudinal structural waves.

Keywords: structural acoustics; Wiener-Hopf technique; acoustic diffraction; flexural wave; elastic shells

1. Introduction

We consider two curved plates, or shells, loaded by a compressible fluid on one side and joined together so that their tangent is continuous along the line of contact. Each shell may have distinct inertial, extensional and flexural characteristics, in addition to the curvature, which can also be discontinuous at the junction. For simplicity we limit this study to the two-dimensional configuration of figure 1. Our objective is a description of the diffraction from the junction, whereby different wave species are generated and scattered into the fluid and the plates. The types of wave interaction include conversion from acoustic to flexural, extensional and acoustic, and the reverse mechanisms. The excitation is an incident structural wave (flexural or longitudinal) or an acoustic plane wave. This paper presents a systematic analytical procedure for their investigation, and provides quantitative predictions of the interactions.

The elastic shells are modelled by two-dimensional thin-shell equations which include explicit coupling between extensional (in-surface) motion and flexural (transverse) motion. Thin-shell theories are well developed and have been used to study the response of fluid-loaded finite bodies, such as the uniform cylinder and sphere. These examples allow of solutions via separable coordinates, whereas finite shell structures

with discontinuities require brute force numerical treatment. Realistic ocean-going structures are composed of piecewise homogeneous sections, or plates, joined along well-defined lines of contact. Individual waves can be identified on large structures, and the question arises as to how such waves interact with the junctions, and how they generate further wave types. Very little is known for arbitrarily curved plates under fluid loading. Two exceptions are the studies by Brazier-Smith (1987) and Norris & Wickham (1995) who considered flexural wave incidence upon the junction of two dissimilar flat plates. The present study contains the flat plate case as a limit in which the coupling between extensional and flexural modes disappears, and only the flexural waves are coupled to the fluid. This leads to a great deal of simplification, in principle, since one can immediately disregard extensional effects. Both studies mentioned presented many useful numerical results and conclusions; in particular, they compared the sensitivity of the acoustic scattering to the type of edge conditions at the junction. This sensitivity to join conditions was also discussed by Wu & Zhu (1995a, b) who extended the work of Brazier-Smith (1987) to include mean flow of the fluid. We restrict attention here to the cases of 'welded' and 'clamped' contact with zero mean flow, although our methodology is easily generalized to other contact conditions. Several authors have discussed diffraction from a surface composed of two semi-infinite impedance strips (Clemmow 1953; Heins & Feshbach 1954; Kay 1959; Senior 1952). This is a further special limiting case of the Brazier-Smith problem, when both plates have vanishing bending stiffnesses. The plates then have only inertial reactions, and the diffraction problem is relatively simple. A complete analysis of this limit is given by Norris & Rebinsky (1995), who also discuss how it can be used to estimate the acoustic-to-extensional diffraction. Rebinsky & Norris (1995a) have also extended this study to include acoustic-to-extensional and shear diffraction.

Unlike the previously mentioned solutions (Brazier-Smith 1987; Senior 1952; etc.), the junction of two distinctly curved shells presents, in general, a non-separable geometry for the acoustic wave equation. We circumvent this difficulty by 'flattening' the plates, or more precisely, the equations, onto the line tangent at the join. This is a reasonable procedure as long as the radii of curvature are large in comparison to the longest wavelength in the problem. Further motivation for the flattening is given in § 3. This still leaves us with a fairly formidable mixed boundary value problem to solve because of the coupling between flexural and extensional motion of the curved plates. The general procedure for attack is to apply Fourier transforms, leading to a Wiener-Hopf problem in the transform parameter. One of the main contributions of this paper is that we provide a systematic procedure to deal with high-order coupled systems of equations which reduce to Wiener-Hopf form. In fact, as we show in § 5, the formal solution is easily found, but the hard work lies in applying the edge conditions. We give a general method for finding the relevant Wiener-Hopf split functions, which again is sufficiently general to cope with far more sophisticated shell theories. Explicit asymptotic forms are obtained for the split functions, which can then be used to reduce the edge conditions to a system of linear equations.

The presentation proceeds in the following sequence, starting with the theory for fluid-loaded curved plates in $\S 2$. Then, in $\S 3$, we apply a 'flattening' approximation to yield a well-defined boundary value problem for a fluid half-space with mixed boundary conditions on a line. Some dispersion functions and reflection coefficients are defined in $\S 4$, after which the formal solution to the boundary value problem

is easily derived and stated in \S 5. Two major hurdles must be surmounted on the way to the solution: first an analytic factorization of the quotient of the dispersion functions must be obtained, and then the join conditions must be satisfied. The former is dealt with in detail in Appendix A, and the join conditions are discussed in \S 6. Satisfaction of these conditions uniquely determines the form of the unknown function in the general solution, hence completing the problem. Several limiting cases are discussed in \S 7, especially the degenerate limiting situations of one plate flat and of both plates flat. In \S 8, we discuss and illustrate the various wave diffraction coefficients along with an examination of energy partition and conservation.

2. General theory

The curved plates of figure 1 may have different densities, elastic properties, thicknesses and curvatures, but they are joined such that the tangent to the surface is continuous across the join. The behaviour of each plate may be described by the dynamic equations for a two-dimensional shell. Let v and w be the in-surface and normal (into the fluid) displacements, and p the total acoustic pressure in the fluid. We consider time-harmonic motion, with $e^{-i\omega t}$ understood but suppressed. The shell equations of motion are

$$\tau_{,s} + m\omega^2 v = 0, (2.1 a)$$

$$\frac{\tau}{b} + Bw_{,ssss} - m\omega^2 w = -p, \quad \text{on } S, \tag{2.1 b}$$

where s is the arc-length and the pressure p is evaluated at the shell S. The shell parameters, b, m, B and C, are constant on each shell, where b is the radius of curvature, m the mass per unit area, B the bending stiffness and C is the extensional stiffness. The latter enters into the constitutive relation for τ , the tensile or longitudinal stress in the plate:

$$\tau = C(v_{,s} + w/b). \tag{2.2}$$

The quantities m, B and C may be related to the intrinsic plate properties; thus, $m = \rho h$, $B = Eh^3/12(1 - \nu^2)$, and $C = Eh/(1 - \nu^2)$, where h, ρ , E and ν are the thickness, density, Young's modulus and Poisson ratio, respectively. The shell equations (2.1) are supplemented by the equation of kinematic continuity between the plate and fluid,

$$\rho_{\rm f}\omega^2 w = \frac{\partial p}{\partial n}, \quad \text{on } S,$$
(2.3)

and the Helmholtz equation in the fluid region $V_{\rm f}$,

$$\nabla^2 p + k_{\rm f}^2 p = 0$$
, in $V_{\rm f}$. (2.4)

Here, $\rho_{\rm f}$ is the fluid density and n is the normal to the surface into the fluid, $k_{\rm f} = \omega/c_{\rm f}$ is the acoustic wave number and $c_{\rm f}$ is the fluid sound speed.

We now reduce the three equations on the surface S, given by equations (2.1) and (2.3), to a single boundary condition. First, define the flexural and longitudinal wave numbers, κ and k, and the impedance length, a, by

$$\kappa^4 = \frac{m}{B}\omega^2, \quad k^2 = \frac{m}{C}\omega^2, \quad a = \frac{m}{\rho_f}.$$
 (2.5)

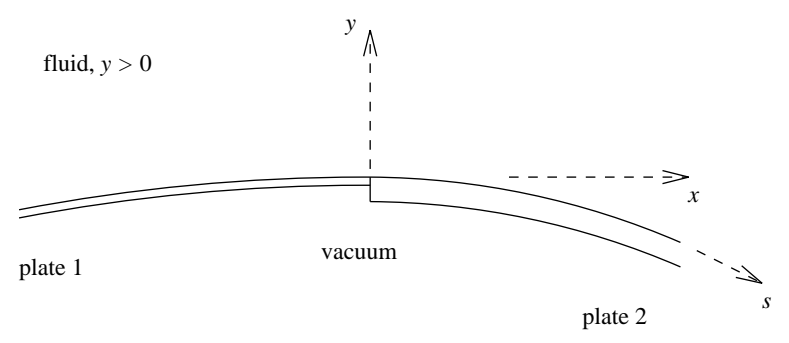


Figure 1. Geometry of the two curved plate structure.

The impedance length is related to the *null frequency* introduced by Crighton *et al.* (1992), defined as the frequency at which $k_{\rm f}a=1$. The null frequency serves as a useful frequency threshold distinguishing the transition from a low-frequency pressure-release regime, to higher frequencies where the plate acts in a more rigid manner. Differentiate the in-surface equation (2.1 a) and use (2.2) to eliminate v, so that the equilibrium condition for in-surface forces becomes

$$\tau_{,ss} + k^2 \tau = \frac{m\omega^2}{b} w. \tag{2.6}$$

The in-surface displacement, now considered as a secondary variable, is

$$v = -(m\omega^2)^{-1}\tau_{.s}. (2.7)$$

Next, eliminate τ from (2.1 b) by operating on the equation with $(\partial_s^2 + k^2)$, yielding

$$\frac{m\omega^2}{b^2}w + (\partial_s^2 + k^2)(Bw_{,ssss} - m\omega^2)w + (\partial_s^2 + k^2)p = 0, \text{ on } S.$$
 (2.8)

Using (2.3) and the definitions (2.5) reduces the boundary condition to a single equation for the pressure:

$$\mathcal{L}p = 0, \quad \text{on } S, \tag{2.9}$$

where the boundary operator is

$$\mathcal{L} \equiv (\partial_s^2 + k^2) + a[(\kappa^{-4}\partial_s^4 - 1)(\partial_s^2 + k^2) + b^{-2}]\partial_n.$$
 (2.10)

Each shell is therefore characterized by the lengths a and b, and the wave numbers k and κ , while the fluid is characterized by its wave number $k_{\rm f}$. One could introduce non-dimensional parameters relative to one of these lengths, preferably $k_{\rm f}^{-1}$, but we choose to maintain the parameters as dimensional. The following non-dimensional parameters for each shell will arise in the sequel where they are explained in more detail: the curvature/flatness relative to the fluid wavelength given by $k_{\rm f}b \gg 1$, the ring frequency, which is the frequency defined by kb=1, the coincidence frequency, defined by $k_{\rm f}=\kappa$, and the previously defined null frequency, at which $k_{\rm f}a=1$. Of these various non-dimensional frequencies we assume that $k_{\rm f}b$ is large, while the remaining parameters can be of any size.

3. Statement of the diffraction problem

A two-dimensional section of a curved shell is shown in figure 1, with fluid above the shell and occupying the half-space y > 0. The surface of the shell is described

locally by $y + x^2/2b \approx 0$ near the origin, and the arc length is $s = x + x^3/6b^2 + \ldots$, or alternatively, $x = s - s^3/6b^2 + \ldots$ Derivatives along the surface may be replaced by derivatives along the tangent x-direction using $\partial_s = (1 - x^2/2b^2 + \ldots)\partial_x$. Similar approximations imply $\partial_n = (1 - x^2/2b^2 + \ldots)\partial_y + (x/b + \ldots)\partial_x$. We now assume that b far exceeds the fluid wavelength, or equivalently, that $\epsilon = (k_{\rm f}b)^{-1}$ is asymptotically small, $\epsilon \ll 1$. Consider a neighbourhood $\mathcal B$ of the origin in which $k_{\rm f}x = O(\epsilon^{-\lambda})$, where $0 < \lambda < \frac{1}{2}$. Within $\mathcal B$ we have $x/b = O(\delta)$, where $\delta = \epsilon^{1-\lambda}$, and hence the partial derivatives ∂_s and ∂_n can be asymptotically approximated as $\partial_s = (1 + O(\delta^2))\partial_x$ and $\partial_n = \partial_y + O(\delta)$. The boundary operator of equation (2.10) becomes $\mathcal L = (1 + O(\delta))\bar{\mathcal L}$, where $\mathcal L$ is the same as $\mathcal L$ but with the tangential and normal derivatives replaced with x- and y-derivatives. Furthermore, to within the same asymptotic approximation, the operator can be defined on y = 0 in the region $\mathcal B$. The same arguments generalize to the case of the two shells joined at x = 0. Thus, we let

$$\epsilon = \max\left(\frac{1}{k_{\rm f}b_{1,2}}\right),\tag{3.1}$$

and again it is explicitly assumed that $\epsilon \ll 1$. The boundary operators approximate in the same way within the region \mathcal{B} , and the continuity conditions for slope, bending moment, etc., approximate accordingly. This local approximation procedure, which is based upon the assumption that shell curvature is much less than the fluid wave number, may be called a shell-flattening approximation. It does not, however, reduce the equations to those of a flat plate under fluid loading, because we still retain the curvature term $1/b^2$ in the 'flattened' operator $\bar{\mathcal{L}}$. This term, which admittedly is small, is the *only* mechanism by which in-surface longitudinal waves can be excited in the shell or radiate into the fluid. Therefore, it is important to retain this term in the equations in order to obtain a quantitative prediction for the mode conversions to and from such membrane waves.

Finally, we note that incident wave fields may be locally approximated in the same manner, in that their values on S can be replaced by their equivalent values on the tangent plane. The relative error is of order $\epsilon^{1-2\lambda} \ll 1$ for a plane acoustic wave incident from the fluid with spatial dependence of the form $\mathrm{e}^{\mathrm{i}k_{\mathrm{f}}(x\cos\theta_0-y\sin\theta_0)}$, where θ_0 is the direction of propagation. This can be seen by expanding the y-phase dependence. Similarly, we can approximate an incident plate wave with dependence like $\mathrm{e}^{\mathrm{i}ks}$ on S. Assuming that the wave number is of the same order as the fluid wave number, which is certainly true of (longitudinal membrane) waves, then a similar analysis for the y-dependence implies that the relative error in the flattening approximation is again of order $\epsilon^{1-2\lambda}$.

The diffraction boundary value problem defined on the joined, curved surface S can therefore be mapped onto an equivalent problem on the tangent plane, as long as the preceding asymptotic reasoning is valid. We assume this to be so for the remainder of the paper, in which case the 'flattened' boundary operator will be denoted by \mathcal{L} , dropping the overbar. In summary, we need to solve the Helmholtz equation (2.4) in the fluid, y > 0, subject to the boundary conditions

$$\left. \begin{array}{ll}
 \mathcal{L}_1 p = 0, & y = 0, & x < 0, \\
 \mathcal{L}_2 p = 0, & y = 0, & x > 0,
 \end{array} \right\}
 \tag{3.2}$$

where

$$\mathcal{L}_{j} \equiv (\partial_{x}^{2} + k_{j}^{2}) + a_{j} [(\kappa_{j}^{-4} \partial_{x}^{4} - 1)(\partial_{x}^{2} + k_{j}^{2}) + b_{j}^{-2}] \partial_{y}, j = 1, 2.$$
(3.3)

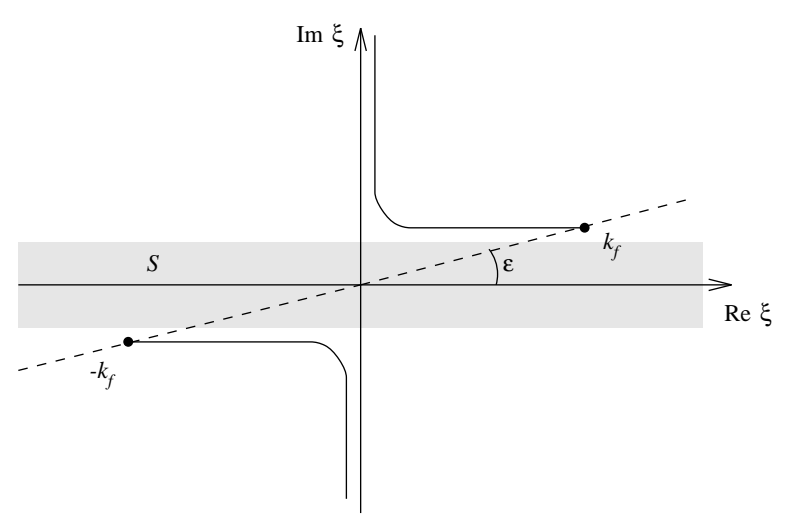


Figure 2. The complex ξ -plane, the branch cuts for $\gamma(\xi)$, and the shaded region $S = \mathcal{H}^+ \cap \mathcal{H}^-$. Note that $\mathcal{H}^+ = S \cup \operatorname{Im} \xi > 0$ and $\mathcal{H}^- = S \cup \operatorname{Im} \xi < 0$.

We will also consider simpler limiting cases of the general equations with fewer junction conditions. The scattering solutions developed in the remainder of the paper provide formally exact answers to the problems posed. They do not take further account of the disparity in the physical parameters, used to 'flatten' the boundary conditions, nor do they take advantage of possible asymptotic approximations in terms of small parameters.

4. The dispersion relation and reflection by a homogeneous plate

(a) Dispersion relation

The dispersion function D associated with the boundary condition operator \mathcal{L} is defined by

$$\mathcal{L}e^{i\xi x - \gamma y} = e^{i\xi x - \gamma y} D(\xi), \tag{4.1}$$

where the radical

$$\gamma(\xi) = (\xi^2 - k_{\rm f}^2)^{1/2} \tag{4.2}$$

is defined as an analytic function in the complex ξ -plane cut as shown in figure 2 so that its imaginary part is non-negative and $\gamma(0) = -ik_f$. Its values along the real axis are

$$\gamma(\xi) = -i\sqrt{k_{\rm f}^2 - \xi^2}, \quad \text{for } |\xi| < k_{\rm f}$$

and

$$\gamma(\xi) = \sqrt{\xi^2 - k_{\rm f}^2}, \text{ for } |\xi| > k_{\rm f}.$$

We have selected this branch for γ so that Fourier superpositions of solutions of the form used in (4.1) are outgoing at infinity. Note also that, for later convenience, we have given k_f a small positive imaginary part, i.e. $k_f = |k_f| e^{i\varepsilon}$, $0 < \varepsilon \ll 1$. We shall further assume that $D(\xi) \neq 0$, $\xi \in \mathcal{H}^+ \cap \mathcal{H}^-$, where \mathcal{H}^{\pm} are upper and lower halves of the complex ξ -plane as shown in figure 2.

The analysis of this paper applies in general to any boundary condition of the form (3.2) with associated dispersion function

$$D(\xi) = U(\xi) - \gamma(\xi)V(\xi). \tag{4.3}$$

The functions U and V are polynomials in ξ^2 with real-valued coefficients, and hence have reflection symmetry in the origin of the complex ξ -plane, i.e. $U(-\xi) = U(\xi)$ and $V(-\xi) = V(\xi)$. For the problem at hand,

$$U(\xi) = k^2 - \xi^2, \quad V(\xi) = U(\xi)\hat{V}(\xi) + a/b^2,$$
 (4.4)

where

$$\hat{V}(\xi) = a(\kappa^{-4}\xi^4 - 1).$$
 (4.5)

Note that U and V are not necessarily irreducible, in the sense that they possess no common polynomial factors. However, $U(\xi)$ is a common factor in the important special case of a flat plate, i.e. when 1/b = 0.

The associated function $D(\xi)$ is defined by

$$\mathcal{L}e^{i\xi x + \gamma y} = e^{i\xi x + \gamma y}\widetilde{D}(\xi), \tag{4.6}$$

and hence

$$\widetilde{D}(\xi) = U(\xi) + \gamma(\xi)V(\xi). \tag{4.7}$$

Thus, D is defined for outgoing wave solutions, and \widetilde{D} for ingoing solutions.

(b) Reflection coefficients

Now suppose a plane wave with incident x-component of slowness ξ_0 impinges on a homogeneous boundary y = 0 where the acoustic pressure satisfies either of (3.2) for all x, then the total field consisting of incident plus reflected waves is

$$p^{(0)}(x,y) = e^{i\xi_0 x + \gamma(\xi_0)y} + R(\xi_0)e^{i\xi_0 x - \gamma(\xi_0)y},$$
(4.8)

where the reflection coefficient

$$R(\xi) = -\frac{\widetilde{D}(\xi)}{D(\xi)}$$

$$= -\frac{U(\xi) + \gamma(\xi)V(\xi)}{U(\xi) - \gamma(\xi)V(\xi)}.$$
(4.9)

Alternatively, we may write this as

$$R(\xi) = -\exp[2\tanh^{-1}(\gamma V/U)].$$
 (4.10)

Thus, $R(-\xi) = R(\xi)$ is complex valued and of unit magnitude for $-k_{\rm f} < \xi < k_{\rm f}$, and R is real for ξ real and $\xi^2 > k_{\rm f}^2$. If the degree of γV equals or exceeds that of U, which is true for the problem under consideration, then $R(\pm \infty) = 1$. Combined with $R(\pm k_{\rm f}) = -1$, this means that there is at least one pair of roots for $R(\xi) = 0$ located on the real axis with $|\xi| > k_{\rm f}$. There may also exist poles of R on the real axis such that $|\xi| > k_{\rm f}$, which are associated with fluid-loaded shell waves, i.e. where $D(\xi) = 0$, and these are discussed below. The reflection coefficient for a plane acoustic wave incident at angle θ from the surface is

$$\mathcal{R}(\theta) = R(k_{\rm f}\cos\theta),\tag{4.11}$$

and hence $|\mathcal{R}(\theta)| = 1$ for real θ .

The reflection coefficients, $R_1(\xi)$ and $R_2(\xi)$, of the individual plates are generally distinct, but they coincide for certain values of the incident wave number. Note that

$$R_1 - R_2 = \frac{2\gamma P^*}{D_1 D_2},\tag{4.12}$$

where P^* is the polynomial

$$P^*(\xi) = U_1(\xi)V_2(\xi) - U_2(\xi)V_1(\xi). \tag{4.13}$$

Hence, if ξ is a root of $P^*(\xi) = 0$, while $D_1(\xi)D_2(\xi) \neq 0$, then $R_1(\xi) = R_2(\xi)$, and both plates reflect equally at such values. We will see that the roots of P^* play a central role in the general solution. Further insight into the physical meaning of these roots can be gained from Appendix C, which discusses a 'sandwich' structure composed of two plates separated by a fluid layer.

If one of the plates is flat, plate 1 say, then $\xi = k_1$ is a simultaneous zero of $P^*(\xi)$ and $D_1(\xi)$, and $R_1(\xi) \neq R_2(\xi)$ in this case. In fact, the flat plate reflection coefficient is independent of the extensional properties, namely

$$R(\xi) = -\frac{1 + \gamma \widehat{V}}{1 - \gamma \widehat{V}}, \quad \text{flat plate.}$$
 (4.14)

(c) Shell waves

Real roots (if any) of the shell dispersion relation

$$D(\xi) = 0 \tag{4.15}$$

correspond to surface wave solutions that can propagate in the absence of any external forcing. There are also complex roots, corresponding to 'leaky' waves (Crighton 1979). Two classes of shell waves may be usefully distinguished, flexural and longitudinal, each of which is unambiguously defined on a flat plate in vacuo. They may be characterized essentially as waves with shell motions which are predominantly transverse, or in-surface, respectively. In the limiting case of the flat plate $(1/b \to 0)$, the root structure simplifies, because D then has the form $D = (1 - \gamma \hat{V})U$, where \hat{V} is defined in (4.5). The dispersion relation for flexural waves on a fluid-loaded flat plate is $1 - \gamma \hat{V} = 0$, and its root structure has been the subject of much discussion in the literature (see, for example, Crighton 1979). This dispersion relation admits of a real root for subsonic flexural waves, which by their nature induce no radiation in the far-field. Generally, we can expect that the flexural roots will be only slightly perturbed from their flat plate values in the presence of shell curvature.

The other possible roots for the flat plate come from $U(\xi) = 0$, or $\xi = \pm k$, which give extensional or longitudinal waves. In the absence of curvature these waves have no transverse motion (w=0) and are not coupled to the fluid. Non-zero curvature causes the roots to be displaced slightly from the real axis, and they can be asymptotically approximated by using the assumption that ϵ of (3.1) is small. The procedure is described by Norris & Rebinsky (1995). The extensional waves are then weakly coupled to the fluid, and are leaky because they are supersonic relative to the acoustic sound speed.

In this paper we will be concerned mainly with frequencies below coincidence. The flexural waves are subsonic and non-radiating but the longitudinal waves are supersonic and leaky, although the 'leakiness' vanishes if the plate is flat. Crighton (1979) has demonstrated quite convincingly that leaky waves have no relevance to the radiated 'far-field' on a flat plate. However, if the waves are weakly leaky, then they may have a large but finite domain of influence (Crighton 1979). This distinction is crucial in dealing with leaky longitudinal waves, because they are by definition only weakly leaky. It can be shown that the loss tangent (ratio of imaginary to real parts of ξ) is of order ϵ^2 (see Norris & Rebinsky 1994). At the same time, the structure being considered usually has a global dimension of the order b, so that the leaky wave can make many circumnavigations before the radiation damping has significantly drained its energy. Thus, the acoustic far-field 'sees' the leaky wave from the entire structure, or more precisely, from those parts of the structure it reaches. At the same time, the concept of 'far-field' is quite different here than in the strictly two-dimensional setting considered by Crighton (1979). We assume the junctions are parts of compact three-dimensional structures, and the far-field is defined in the sense appropriate to this situation. Bearing these distinctions in mind, it should be clear that the leaky longitudinal waves are of utmost significance as far as the far-field is concerned. We note that the poles giving the leaky longitudinal waves lie on the unphysical Riemann sheet, which is discussed further in Appendix A.

5. Formal solution of the diffraction problem

(a) Incident and scattered fields

We now consider the scattering problem defined in § 3. First, we introduce the scattered field $p^{(s)}$ according to

$$p(x,y) = p^{(0)}(x,y) + p^{(s)}(x,y), (5.1)$$

where $p^{(0)}$ is an incident wave solution with horizontal wave number ξ_0 and satisfying the boundary condition on x < 0. Thus, $p^{(0)}$ may be an incident plane acoustic wave with $\xi_0 = k_f \cos \theta_0$, where $0 < \theta_0 < \frac{1}{2}\pi$ so that ξ_0 lies in the upper half-plane, and the amplitude of $p^{(0)}$ at the origin is then $(1 + \mathcal{R}_1(\theta_0))$ times the incident pressure there. Or, it could be an incident-free shell wave, in which case ξ_0 is a root of the dispersion equation (4.15) with $\text{Re }\xi_0 > 0$. The flat plate presents a special case, for, if plate 1 is flat and the incident wave is an extensional (longitudinal) wave, then the associated incident pressure is zero. We denote this as an FPL wave (flat plate, longitudinal) and say more about it later. Thus, the incident field is assumed to be

of the form

$$p^{(0)}(x,y) = e^{i\xi_0 x} \begin{cases} [e^{\gamma(\xi_0)y} + R_1(\xi_0)e^{-\gamma(\xi_0)y}], & \text{acoustic wave,} \\ e^{-\gamma(\xi_0)y}, & \text{shell wave,} \\ 0, & \text{FPL wave.} \end{cases}$$
(5.2)

We assume for FPL incidence that the incident stress, $\tau^{(0)}(x)$, defined by analogy with (5.1), is of the form

$$\tau^{(0)}(x) = e^{i\xi_0 x}, \quad \xi_0 \equiv k_1, \quad \text{FPL wave.}$$
 (5.3)

Without loss of generality, we may suppose that ξ_0 lies in the upper half, \mathcal{H}^+ , of the complex ξ -plane described in figure 2. One could use spectral superposition to consider more complicated incident wave fields, but we restrict attention in this paper to plane acoustic and shell waves.

The boundary conditions (3.2) may then be written as

We now introduce an outgoing Fourier superposition of plane waves for $p^{(s)}$ in the form

$$p^{(s)}(x,y) = \frac{1}{2\pi} \int_{-\infty}^{\infty} \tilde{p}(\xi) e^{i\xi x - \gamma(\xi)y} d\xi.$$
 (5.5)

This will satisfy (5.4) if the dual equations

$$\frac{1}{2\pi} \int_{-\infty}^{\infty} D_1(\xi) \tilde{p}(\xi) e^{i\xi x} d\xi = 0, \quad x < 0,$$
 (5.6 a)

$$\frac{1}{2\pi} \int_{-\infty}^{\infty} D_2(\xi) \tilde{p}(\xi) e^{i\xi x} d\xi = -D_2(\xi_0) A_0 e^{i\xi_0 x}, \quad x > 0,$$
 (5.6 b)

hold with

$$A_0 = \begin{cases} R_1(\xi_0) - R_2(\xi_0), & \text{acoustic wave,} \\ 1, & \text{shell wave,} \\ (k_2^2 - k_1^2)/[b_2 D_2(k_1)], & \text{FPL wave,} \end{cases}$$
 (5.7)

where the FPL result follows from equations (2.1) and (5.3). Note that $A_0 = 0$ for plane wave incidence if ξ_0 is a root of $P^* = 0$, (but not a root of $D_1D_2 = 0$, cf. equation (4.13)), in which case the scattered pressure is identically zero. A_0 also vanishes for FPL incidence if $k_2 = k_1$, even when plate 2 is not flat $(1/b_2 \neq 0)$. We call this highly degenerate but physically significant configuration FPL*. There is still a scattered pressure in this case, and it turns out that the analysis is essentially the same whether A_0 vanishes or not. We discuss the FPL* case in more detail later in § 7.

(b) General solution

It is evident that (5.6 a) is satisfied by writing

$$\tilde{p}(\xi) = F^{-}(\xi)/D_1(\xi),$$
(5.8)

where F^- is any function analytic in \mathcal{H}^- and

$$F^{-}(\xi) = O(\xi^{-1}), \quad \xi \to \infty, \quad \xi \in \mathcal{H}^{-}. \tag{5.9}$$

Substituting this ansatz into the second of (5.6) yields

$$\frac{1}{2\pi} \int_{-\infty}^{\infty} \frac{D_2(\xi)}{D_1(\xi)} F^-(\xi) e^{i\xi x} d\xi = -D_2(\xi_0) A_0 e^{i\xi_0 x}, \quad x > 0.$$
 (5.10)

Again by inspection, a particular solution of this equation is

$$F^{-}(\xi) = \frac{iA_0 D_2(\xi_0)}{\xi - \xi_0} \frac{K^{-}(\xi)}{K^{+}(\xi_0)},\tag{5.11}$$

where

$$K(\xi) = \frac{D_1(\xi)}{D_2(\xi)} = \frac{K^-(\xi)}{K^+(\xi)}.$$
 (5.12)

That is, $K^{\pm}(\xi)$ are particular Wiener–Hopf factors of the quotient of the two dispersion functions that are analytic in the half-planes \mathcal{H}^{\pm} of figure 2.

A little reflection on the preceding argument shows that further solutions of the dual equations may be generated according to the prescription

$$F^{-}(\xi) = \frac{\mathrm{i}A(\xi)D_2(\xi_0)}{\xi - \xi_0} \frac{K^{-}(\xi)}{K^{+}(\xi_0)},\tag{5.13}$$

where $A(\xi)$ is now a polynomial of degree no greater than q (say) where q is chosen so that (5.9) is satisfied in the whole complex plane and

$$A(\xi_0) = A_0. (5.14)$$

The general solution for the pressure transform is

$$\tilde{p}(\xi) = \frac{iA(\xi)}{\xi - \xi_0} \frac{G(\xi_0)}{G(\xi)},\tag{5.15}$$

where G is an analytical generalization of the dispersion functions,

$$G(\xi) \equiv \frac{D_2(\xi)}{K^+(\xi)} = \frac{D_1(\xi)}{K^-(\xi)}.$$
 (5.16)

Thus we have provided a formal construction of a q-parameter family of outgoing scattered fields satisfying Helmholtz's equation and the shell boundary conditions (3.2). It remains to satisfy the conditions at the junction of the two plates. Evidently, the value of q depends only on the size of the factors K^{\pm} as $\xi \to \infty$, and we would expect that the physical constraints at the join associated with a particular form for $D(\xi)$ will also number q to enable a unique construction. In §6 we shall show that this is indeed the case, after we provide an analytic construction for $K^{\pm}(\xi)$ in Appendix A. But first, we discuss the general form of the solutions for the other physical quantities of interest.

(c) Displacement and stress solutions

The pressure, the transverse and in-plane deflections, and the membrane stress may all be expressed in terms of two fundamental potentials $p_0(x)$, and $w_0(x)$,

$$p(x,y) = p^{(0)}(x,y) - A\left(-i\frac{\partial}{\partial x}\right)p_0(x,y), \tag{5.17a}$$

$$\rho_{\rm f}\omega^2 w(x) = \frac{\partial p^{(0)}}{\partial y}(x,0) - A\left(-i\frac{\mathrm{d}}{\mathrm{d}x}\right)w_0(x),\tag{5.17b}$$

$$\frac{\tau(x)}{b} = -p^{(0)}(x,0) - a\left(\frac{1}{\kappa^4}\frac{\partial^4}{\partial x^4} - 1\right)\frac{\partial p^{(0)}}{\partial y}(x,0) - A\left(-i\frac{\mathrm{d}}{\mathrm{d}x}\right)\tau_0(x), \quad (5.17c)$$

$$v(x) = -\frac{1}{m\omega^2} \frac{\mathrm{d}\tau}{\mathrm{d}x},\tag{5.17d}$$

where

$$p_0(x,y) = \frac{1}{2\pi i} \int_{-\infty}^{\infty} \frac{G(\xi_0)}{G(\xi)} \frac{e^{i\xi x - \gamma y}}{\xi - \xi_0} d\xi,$$
 (5.18 a)

$$w_0(x) = -\frac{1}{2\pi i} \int_{-\infty}^{\infty} \gamma(\xi) \frac{G(\xi_0)}{G(\xi)} \frac{e^{i\xi x}}{\xi - \xi_0} d\xi, \qquad (5.18 b)$$

and $p_0(x,0)$ is denoted by $p_0(x)$. The function $\tau_0(x)$ depends upon $w_0(x)$, $p_0(x)$ and the plate parameters,

$$\tau_0(x) = -p_0(x) - a\left(\frac{1}{\kappa^4} \frac{d^4}{dx^4} - 1\right) w_0(x).$$
 (5.19)

As is usual, the material parameters take the appropriate values either side of the join at x=0. These relations follow from equations (5.1), (5.5), (5.15), (2.1b), (2.3) and (2.7). At first, it may appear to be a simple matter to formally apply the junction continuity conditions by using the above expressions for p, w, τ and v. However, (5.18b) will in general have weak singularities at x=0 and it is therefore necessary to proceed with caution. Our approach is straightforward in that we will first derive alternative expressions for $p_0(x)$ and $w_0(x)$ so that it is easy to find their power series as $x\to 0^\pm$ and then obtain an algebraic system of equations for the undetermined coefficients in A by substituting these expansions into (5.17) and the junction conditions.

(d) Diffraction coefficients

The scattered pressure simplifies at distances far from the junction in units of the longest wavelength in the problem. A far-field approximation may be obtained by the usual methods of first shifting the contour of integration from the real axis to the path of steepest descents. The saddle point then yields the scattered pressure in the fluid, which depends upon a diffraction coefficient $C(\theta)$ defined such that

$$p^{(s)} = C(\theta) \sqrt{\frac{2}{\pi k_f r}} e^{-i\pi/4} e^{ik_f r}, \quad k_f r \to \infty, \quad 0 < \theta \leqslant \pi,$$
 (5.20)

where

$$C(\theta) = \frac{1}{2}k_{\rm f}\sin\theta\,\tilde{p}(k_{\rm f}\cos\theta). \tag{5.21}$$

If the incident wave is an acoustic wave with angle of incidence θ_0 such that $\xi_0 = k_f \cos \theta_0$, the diffraction coefficient can be considered a function of both angles, i.e. $C(\theta, \theta_0)$. It follows from (5.7), (5.15) and (5.21) as

$$C(\theta, \theta_0) = -\frac{1}{2}\gamma(\xi) \frac{G(\xi_0)}{G(\xi)} \frac{A(\xi, \xi_0)}{\xi - \xi_0},$$
(5.22)

where $\xi = k_{\rm f} \cos \theta$ and we have rewritten $A(\xi)$ as $A(\xi, \xi_0)$ to remind us that it is a function of both the incident and scattered directions.

When the observation angle θ is close to $\theta = 0$, the deformation onto the path of steepest descents will capture two poles which correspond to the subsonic flexural wave and supersonic longitudinal wave travelling to the right in x > 0. The flexural pole occurs at the positive real zero of $D_2(\xi)$. The longitudinal pole is actually a root of $D_2(\xi)$ with real positive part less than k_f and a small positive imaginary part. Note that the longitudinal wave has Re $\gamma < 0$, but for some values of x and y the phase $i\xi x - \gamma y$ represents an outgoing wave. In order to capture the longitudinal pole, the contour must be deformed onto the other Riemann sheet represented by Re $\gamma < 0$. Whether or not the longitudinal pole is captured depends upon the position of the point of stationary phase. A discussion of similar contour manipulations can be found in the works of Crighton (1971) and Rebinsky & Harris (1992). Similarly, when θ is close to $\theta = \pi$, the deformation of the contour captures poles at the zeros of $D_1(\xi)$ and $D_1(\xi)$ corresponding to the negative counterparts of those for x>0. For example, when the incident field is a subsonic flexural wave advancing from the left, the residues at these poles are the reflected and transmitted waves, respectively. Using equations (5.15) and (5.16) with $\xi_0 = \xi_s^{(1)}$ (the subscript 's' indicating the subsonic flexural root), we thus find the left- and right-going waves are

$$p_1 = R_{\text{flex}} e^{-i\xi_s^{(1)} x - \gamma(\xi_s^{(1)})y} + R_{\text{long}} H(-\theta_1 - \theta) e^{-i\xi_m^{(1)} x - \gamma(\xi_m^{(1)})y},$$
 (5.23 a)

$$p_2 = T_{\text{flex}} e^{i\xi_s^{(2)}x - \gamma(\xi_s^{(2)})y} + T_{\text{long}} H(\theta_2 - \theta) e^{i\xi_m^{(2)}x - \gamma(\xi_m^{(2)})y},$$
(5.23b)

where $\xi_{\rm s}^{(1)}$, $\xi_{\rm m}^{(1)}$ and $\xi_{\rm s}^{(2)}$, $\xi_{\rm m}^{(2)}$ are the wave numbers of the subsonic flexural and membrane waves on the right- and left-hand plates, respectively. Also, H is the Heaviside function, $\theta = \tan^{-1}(y/x)$, and $\theta_{1,2} \approx \sin^{-1}(k_{1,2}/k_{\rm f})$ which are the longitudinal wave critical angles. The reflection and transmission coefficients for the subsonic flexural waves are

$$R_{\text{flex}} = \frac{A(-\xi_{\text{s}}^{(1)})G(\xi_{\text{s}}^{(1)})}{2\xi_{\text{s}}^{(1)}K^{+}(\xi_{\text{s}}^{(1)})D'_{1}(\xi_{\text{s}}^{(1)})}, \quad T_{\text{flex}} = \frac{A(\xi_{\text{s}}^{(2)})G(\xi_{\text{s}}^{(1)})K^{+}(\xi_{\text{s}}^{(2)})}{(\xi_{\text{s}}^{(1)} - \xi_{\text{s}}^{(2)})D'_{2}(\xi_{\text{s}}^{(2)})}, \quad (5.24)$$

respectively. Note that the polynomial $A(\xi)$ is also a function of the incident direction, given in this example as $\xi_s^{(1)}$, in addition to the scattered direction. We can also determine those coefficients describing the diffracted longitudinal waves, both reflected and transmitted,

$$R_{\text{long}} = \frac{A(-\xi_{\text{m}}^{(1)})G(\xi_{\text{s}}^{(1)})}{(\xi_{\text{s}}^{(1)} + \xi_{\text{m}}^{(1)})K^{+}(\xi_{\text{m}}^{(1)})D_{1}'(\xi_{\text{m}}^{(1)})}, \quad T_{\text{long}} = \frac{A(\xi_{\text{m}}^{(2)})G(\xi_{\text{s}}^{(1)})K^{+}(\xi_{\text{s}}^{(2)})}{(\xi_{\text{s}}^{(1)} - \xi_{\text{m}}^{(2)})D_{2}'(\xi_{\text{m}}^{(2)})}, \quad (5.25)$$

respectively. Note that the diffraction coefficients of (5.24) and (5.25) are in terms of the surface pressure, not the displacement.

(e) Consequences of reciprocity

Acoustical reciprocity requires that the diffraction should be the same under the interchange of the source and receiver directions, or

$$C(\theta, \theta_0) = C(\pi - \theta_0, \pi - \theta). \tag{5.26}$$

This implies, using (5.22),

$$A(\xi, \xi_0)\gamma(\xi)G(\xi_0)/G(\xi) = A(-\xi_0, -\xi)\gamma(\xi_0)G(-\xi)/G(-\xi_0),$$
 (5.27)

where we have written $A(\xi)$ as $A(\xi, \xi_0)$ to remind us that it is a function of both incident and scattered directions. Now,

$$G(\xi)G(-\xi) = D_1(\xi)D_2(\xi) = \frac{2\gamma(\xi)P^*(\xi)}{R_1(\xi) - R_2(\xi)},$$
(5.28)

from (4.12), (5.16) and (A 1), while the denominator in the last expression simplifies further for acoustic wave incidence as $R_1(\xi) - R_2(\xi) = A(\xi, \xi)$, from (5.7). Using (5.27) and (5.28) and the identity $A(\xi, \xi) = A(-\xi, -\xi)$, we see that reciprocity implies the connection

$$A(\xi,\xi)A(-\xi,\xi_0)P^*(\xi_0) = A(\xi_0,\xi_0)A(-\xi_0,\xi)P^*(\xi).$$
(5.29)

The function A must satisfy this relation for arbitrary plane wave incidence.

(f) Energy conservation

The balance of wave power, or flux, can be used as a check on the solution of the fluid-curved plate system. The energy conservation identity for flat plates has been previously studied by Crighton & Innes (1984) and by Norris & Wickham (1995). Here we require the energy flux (the structural intensity) for a curved plate under unilateral fluid loading. A general theorem on energy for an inhomogeneous elastic shell with fluid loading was derived by Pierce (1993), with the final form given by

$$\frac{\partial \mathcal{E}}{\partial t} + D_{\alpha} I^{\alpha} = -p w_{,t}, \tag{5.30}$$

where \mathcal{E} is the total energy and I^{α} is the structural intensity. Following Crighton & Innes (1984), we take the time average of (5.30) to obtain

$$\langle I^{1}(x_{1}) - I^{1}(x_{2}) \rangle = \left\langle \int_{S} pw_{,t} \, \mathrm{d}x \right\rangle, \tag{5.31}$$

with

$$I^{1} = -\tau v_{,t} - B(w_{,xx}w_{,xt} - w_{,xxx}w_{,t}), \tag{5.32}$$

being the remaining component of the structural intensity and S the surface in the fluid joining the points x_1 and x_2 on the plate. The time average in equation (5.31) is defined by

$$\langle f_1(x_1,t)f_2(x_1,t)\rangle = \frac{1}{2}\operatorname{Re}[f_1(x_1)f_2^*(x_1)],$$
 (5.33)

where * denotes complex conjugation. The time average of the structural intensity I^1 is given by

$$\langle I^1 \rangle = \frac{1}{2} \operatorname{Re}[-i\omega B(w_{.xxx}^* w - w_{.xx}^* w_{.xt}) + i\omega \tau^* v].$$
 (5.34)

In addition to the structural intensity one must also determine the rate of working of the pressure, which is given by

$$\langle I_p \rangle = \frac{1}{2} \operatorname{Re} \left[\int_0^\infty p \left(\frac{1}{\mathrm{i}\rho_{\mathrm{f}}\omega} \frac{\partial p}{\partial x} \right)^* \mathrm{d}y \right].$$
 (5.35)

The sum of these contributions gives the total energy flux $\mathcal F$ associated with the structural wave.

For the longitudinal wave this is simply just the energy flux in the curved plate,

$$\mathcal{F}_{\text{long}} = L(\xi_{\text{m}}) \frac{|\tau_0|^2}{2m\omega} e^{-2\delta_{\text{m}}|x|},$$

$$L(\xi_{\text{m}}) = \text{Re}(\xi_{\text{m}}) (1 + 2 \operatorname{Re}(\xi_{\text{m}}^*)^2 |U(\xi_{\text{m}})|^2 b^2 \kappa^{-4}), \tag{5.36}$$

where τ_0 is the incident stress amplitude, $\xi_{\rm m}$ is the longitudinal wave number in the curved plate and $\delta_{\rm m}={\rm Im}\,\xi_{\rm m}$. Note that at $x=\pm\infty$ the longitudinal flux in the curved plate is zero. Here we will assume that this expression is approximately valid at x=0 when using far-field diffraction coefficients. The longitudinal pressure coefficients (5.25) can be converted to stress-based coefficients by multiplying by the factor $b(1+\gamma\widehat{V})$:

$$R_{\text{long}}^{\tau} = b_1 [1 + \gamma(\xi_{\text{m}}^{(1)}) \hat{V}_1(\xi_{\text{m}}^{(1)})] R_{\text{long}}, \tag{5.37 a}$$

$$T_{\text{long}}^{\tau} = b_2 [1 + \gamma(\xi_{\text{m}}^{(2)}) \hat{V}_2(\xi_{\text{m}}^{(2)})] T_{\text{long}},$$
 (5.37 b)

where γ has been negated to account for the longitudinal poles being on the lower sheet (Re $\gamma < 0$) of the complex ξ -plane. The energy flux for the longitudinal waves can be obtained in terms of pressure by using equations (2.3) and (2.6) to relate the stress to the pressure. Then

$$\frac{|\tau_0|^2}{2m\omega} = \frac{a}{b^2} \frac{|\gamma(\xi_{\rm m})|^2}{|U(\xi_{\rm m})|^2} \frac{|p_0|^2}{2\rho_{\rm f}\omega}.$$
 (5.38)

The flux for a flat plate is obtained from equation (5.36) by letting $b \to \infty$ and noting that in this limit $U(\xi_{\rm m}) \to 1/b^2$.

The subsonic flexural wave contains energy in both the curved plate and the fluid. After some algebraic manipulations using equations (5.34) and (5.35), the flux is

$$\mathcal{F}_{\text{flex}} = F(\xi_s) \frac{|p_0|^2}{2\rho_f \omega},$$

$$F(\xi_s) = -\frac{D'(\xi_s)\gamma(\xi_s)}{2U(\xi_s)} = a\xi_s \gamma^2(\xi_s) \left(2\frac{\xi_s^2}{\kappa^4} + \frac{1}{U^2(\xi_s)b^2}\right) + \frac{\xi_s}{2\gamma(\xi_s)},$$
(5.39)

where ξ_s is the subsonic flexural wave number. Once again the expression for a flat plate follows by letting $b \to \infty$.

The flux of acoustic energy diffracted from the junction into the fluid follows from (5.20) as

$$\lim_{r \to \infty} \frac{1}{\rho_{\rm f} c_{\rm f}} \int_0^{\pi} |p^{(\rm s)}(r,\theta)|^2 r \, \mathrm{d}\theta = \frac{2}{\pi \rho_{\rm f} \omega} \int_0^{\pi} |C(\theta)|^2 \, \mathrm{d}\theta.$$
 (5.40)

Now consider an incident flexural wave with unit flux, then equations (5.36)–(5.40) may be combined to provide a statement of energy conservation. We will find that subsonic flexural waves provide the only means of significant energy flow away from

the junction, other than acoustic diffraction loss (cf. §8). Note that the membrane (longitudinal) waves are leaky so that at large distances from the junction their energy flux is zero. Applying the above energy flux identities at the junction gives

$$1 = |R_{\text{flex}}|^2 + \frac{F^{(2)}(\xi_{\text{f}}^{(2)})}{F^{(1)}(\xi_s^{(1)})} |T_{\text{flex}}|^2 + \frac{1}{a_1} \frac{L^{(1)}(\xi_{\text{m}}^{(1)})}{F^{(1)}(\xi_s^{(1)})} |R_{\text{long}}^{\tau}|^2 + \frac{1}{a_2} \frac{L^{(2)}(\xi_{\text{m}}^{(2)})}{F^{(1)}(\xi_s^{(1)})} |T_{\text{long}}^{\tau}|^2 + \frac{1}{F^{(1)}(\xi_s^{(1)})} \frac{4}{\pi} \int_0^{\pi} |C(\theta)|^2 d\theta. \quad (5.41)$$

The five terms on the right-hand side are each positive and less than unity, and correspond to the fractional energy reflected as flexural on plate 1, transmitted as flexural on plate 2, reflected as longitudinal on plate 1, transmitted as longitudinal on plate 2 and acoustically radiated into the fluid. A similar equation can be obtained for longitudinal wave incidence.

6. Satisfying the join conditions

We now give a general systematic procedure for evaluating $A(\xi)$ in the formal solution (5.15) so that various prescribed conditions at the junctions of the plates may be determined. We shall proceed in the context of the problem posed in §3, but the reader should notice that the analysis is valid for a wide class of plate models and physical constraints at the join. Application of the junction conditions requires knowledge of the behaviour of the potentials $p_0(x)$ and $w_0(x)$ in the neighbourhood of the join, x = 0. Our first order of business is to obtain analytic expansions of these quantities; actually, as we will see, Taylor series in x. We can then apply the conditions in a straightforward manner.

(a) Alternative integral forms for w_0 and p_0

The potentials are both in the form of Fourier transforms which can be separated into two distinct transforms each of which vanishes for either x > 0 or x < 0. Thus,

$$\{p_{0}(x), w_{0}(x)\} = \frac{1}{2\pi i} \int_{-\infty}^{\infty} \{\tilde{p}_{0}(\xi), \tilde{w}_{0}(\xi)\} e^{i\xi x} d\xi$$
$$= \frac{1}{2\pi i} \int_{-\infty}^{\infty} \{\tilde{p}_{0}^{\pm}(\xi), \tilde{w}_{0}^{\pm}(\xi)\} e^{i\xi x} d\xi, \quad x \leq 0,$$
(6.1)

where \tilde{w}_0^+ , \tilde{w}_0^- , are the analytic partitions of \tilde{w}_0 , defined by

$$\tilde{w}_0(\xi) = \tilde{w}_0^+(\xi) + \tilde{w}_0^-(\xi), \tag{6.2}$$

such that $\tilde{w}_0^+(\xi)$ is analytic in \mathcal{H}^+ and $\tilde{w}_0^-(\xi)$ is analytic in \mathcal{H}^- . Analytic partitions of $\tilde{p}_0(\xi)$ are defined in the same manner. The transforms \tilde{w}_0 and \tilde{p}_0 , as defined in equation (5.18), may be rewritten by noting that

$$\gamma(\xi)/G(\xi) = [K^{-}(\xi)U_2(\xi) - K^{+}(\xi)U_1(\xi)]/P^{*}(\xi), \tag{6.3 a}$$

$$1/G(\xi) = [K^{-}(\xi)V_2(\xi) - K^{+}(\xi)V_1(\xi)]/P^{*}(\xi), \tag{6.3b}$$

which are easily obtained by eliminating γ between the two equations (5.16). Thus,

$$\tilde{w}_0(\xi) = G(\xi_0) \frac{U_1(\xi)K^+(\xi) - U_2(\xi)K^-(\xi)}{(\xi - \xi_0)P^*(\xi)},$$
(6.4 a)

$$\tilde{p}_0(\xi) = -G(\xi_0) \frac{V_1(\xi)K^+(\xi) - V_2(\xi)K^-(\xi)}{(\xi - \xi_0)P^*(\xi)},$$
(6.4 b)

where the denominator in these integrands is the polynomial P^* defined in equation (4.13). The general form of the polynomial is

$$P^*(\xi) = P_0^* \prod_{n=1}^{N^*/2} (\xi^2 - \zeta_n^2), \tag{6.5}$$

say, where the zeros $\pm \zeta_n$, $n=1,2,\ldots,\frac{1}{2}N^*$ are necessarily outside $\mathcal{H}^+\cap\mathcal{H}^-$, and we define them such that $\zeta_n, n=1,2,\ldots,\frac{1}{2}N^*$ are in \mathcal{H}^+ . For the problem under consideration

$$N^* = 8$$
 and $P_0^* = \frac{a_2}{\kappa_2^4} - \frac{a_1}{\kappa_1^4}$. (6.6)

The partition functions can be found quite easily from (6.4) because, apart from the split function K^+ and K^- , the only singularities arise from the simple poles at $\xi = \xi_0$ and the roots of $P^* = 0$. By adding and subtracting poles at the same points with suitable residues, we can arrive at explicit formulae for the partitioned functions. They therefore become

$$\tilde{w}_{0}^{-}(\xi) = G(\xi_{0}) \left\{ \frac{U_{1}(\xi_{0})K^{+}(\xi_{0})}{(\xi - \xi_{0})P^{*}(\xi_{0})} - \frac{U_{2}(\xi)K^{-}(\xi)}{(\xi - \xi_{0})P^{*}(\xi)} + \sum_{n=1}^{4} \left[\frac{u_{1n}^{+}}{(\xi - \zeta_{n})(\zeta_{n} - \xi_{0})} + \frac{u_{2n}^{-}}{(\xi + \zeta_{n})(-\zeta_{n} - \xi_{0})} \right] \right\}, \quad (6.7 a)$$

$$\tilde{w}_{0}^{+}(\xi) = G(\xi_{0}) \left\{ \frac{U_{1}(\xi)K^{+}(\xi)}{(\xi - \xi_{0})P^{*}(\xi)} - \frac{U_{1}(\xi_{0})K^{+}(\xi_{0})}{(\xi - \xi_{0})P^{*}(\xi_{0})} - \sum_{n=1}^{4} \left[\frac{u_{1n}^{+}}{(\xi - \zeta_{n})(\zeta_{n} - \xi_{0})} + \frac{u_{2n}^{-}}{(\xi + \zeta_{n})(-\zeta_{n} - \xi_{0})} \right] \right\}, \quad (6.7 b)$$

where

$$u_{jn}^{\pm} = \text{residue of } \left[\frac{U_j(\xi)K^{\pm}(\xi)}{P^*(\xi)} \right]_{\xi = \pm \zeta_n}.$$
 (6.8)

The functions \tilde{p}_0^+ and \tilde{p}_0^- then follow by simply replacing U_j with $-V_j$, j=1,2, in equations (6.7) and (6.8). The residues u_{1n}^+ and u_{2n}^- can be related to one another by noting, from equations (4.13), (5.16) and (6.3), that

$$K = \frac{U_1}{U_2} = \frac{V_1}{V_2}, \quad \text{at } \xi = \pm \zeta_n.$$
 (6.9)

This identity, together with the fact that P^* is an even function, implies

$$u_{2n}^{-} = -u_{1n}^{+}/[K^{-}(\zeta_n)K^{+}(\zeta_n)], \tag{6.10}$$

for each n.

(b) Behaviour of w_0 and p_0 near the join

In practice, to satisfy the join conditions, we only need the asymptotic forms for p_0 and w_0 and their derivatives near x=0, and these follow immediately from the power series expansion of the Fourier transform about the point at infinity. For instance, let f signify either of these functions, and suppose that the partitions of $\tilde{f}(\xi)$ are of the form

$$\tilde{f}^{\pm}(\xi) = \mp \sum_{m=1}^{M} \tilde{f}_{m-1}^{\mp} \xi^{-m} + O(\xi^{-(M+1)} \log \xi), \tag{6.11}$$

for some integer $M \ge 1$. Then it can be shown that

$$f(x) = \sum_{m=0}^{M} \tilde{f}_{m}^{\pm} \frac{(\mathrm{i}x)^{m}}{m!} + O(x^{M} \log|x|), \quad x \leq 0.$$
 (6.12)

The only terms containing logarithmic singularities in the expressions (6.7) for \tilde{w}_0^{\pm} are those with $K^{\pm}(\xi)$, respectively. Referring to the asymptotic results in equations (B 6) and (B 7), and to equations (6.5)–(6.7), the leading-order singular term at infinity in the expansion of the Fourier transforms for w_0 in (6.1) is of order $\xi^{-12} \log \xi$. On inversion, the latter yields a term of order $x^{11} \log |x|$. Similarly, the transforms for p_0 have a leading-order singularity of order $\xi^{-8} \log \xi$, yielding a term of order $x^7 \log |x|$. The leading-order singularities for the stress $\tau(x)$ and the inplane displacement v(x) depend upon the function $\tau_0(x)$ of equation (5.19), with the associated transform (cf. (4.5))

$$\tilde{\tau}_0(\xi) = -\tilde{p}_0(\xi) - \hat{V}(\xi)\tilde{w}_0(\xi).$$
 (6.13)

Hence, for example, the transform required to evaluate $\tau_0(x)$ for x < 0 is

$$\tilde{\tau}_0(\xi) = -\{U_1(\xi)\tilde{p}_0^+(\xi) + [V_1(\xi) - a_1/b_1^2]\tilde{w}_0^+(\xi)\}/U_1(\xi), \tag{6.14}$$

which, from (6.7) and the corresponding equation for \tilde{p}_0^+ , has a singularity of the form $\xi^{-14} \log \xi$. The leading-order singularity of $\tau_0(x)$ is therefore $x^{13} \log |x|$. The transforms \tilde{w}_0^{\pm} and \tilde{p}_0^{\pm} may be put into the form (6.11), where, based upon

The transforms \tilde{w}_0^{\pm} and \tilde{p}_0^{\pm} may be put into the form (6.11), where, based upon the above discussion, M=7 and 11, respectively. The details of the splitting can be found in Appendix B. Having expanded the transforms about the point at infinity it is a simple matter to invert term by term by using equation (6.12), which yields explicit power series for $w_0(x)$ and $p_0(x)$ near the origin, namely

$$w_0(x) = \sum_{n=0}^{11} \lambda_n^{\pm} \frac{(ix)^n}{n!} + O(x^{11} \log |x|), \quad x \leq 0,$$
 (6.15 a)

$$p_0(x) = \sum_{n=0}^{7} \psi_n^{\pm} \frac{(ix)^n}{n!} + O(x^7 \log|x|), \quad x \leq 0,$$
 (6.15b)

and, again, the coefficients are listed explicitly in Appendix B. We note that $\lambda_j^+ = \lambda_j^-$ for j = 0–5, and hence $w_0(x)$ and its first five derivatives are continuous at x = 0. Similarly, $\psi_0^+ = \psi_0^-$ and $\psi_1^+ = \psi_1^-$, implying that $p_0(x)$ and $\mathrm{d} p_0(x)/\mathrm{d} x$ are continuous at x = 0.

(c) Determination of $A(\xi)$

Letting

$$A(\xi) = \sum_{n=0}^{q} \bar{A}_n \xi^n,$$
 (6.16)

we see that equation (5.14) implies the identity

$$\sum_{n=0}^{q} \bar{A}_n \xi_0^n = A_0. \tag{6.17}$$

The displacement and pressure near the origin therefore follow from equations (5.17), (6.15) and (6.17), as

$$\rho_{\rm f}\omega^2 w(x) = \frac{\partial p^{(0)}}{\partial y}(x,0) - \sum_{n=0}^{11-q} \Lambda_n^{\pm} \frac{(\mathrm{i}x)^n}{n!} + O(x^{11-q}\log|x|), \quad x \leq 0, \tag{6.18a}$$

$$p(x,0) = p^{(0)}(x,0) - \sum_{n=0}^{7-q} \Psi_n^{\pm} \frac{(\mathrm{i}x)^n}{n!} + O(x^{7-q} \log|x|), \quad x \leq 0,$$
 (6.18b)

where

$$\Lambda_n^{\pm} = \sum_{k=0}^{q} \bar{A}_k \lambda_{k+n}^{\pm} H(11 - k - n), \tag{6.19 a}$$

$$\Psi_n^{\pm} = \sum_{k=0}^q \bar{A}_k \psi_{k+n}^{\pm} H(7 - k - n), \tag{6.19 b}$$

and H indicates the Heaviside step function with H(0) = 1. The stress and velocity depend upon

$$A\left(-i\frac{\mathrm{d}}{\mathrm{d}x}\right)\tau_0(x) = \Gamma_0^{\pm} + ix\Gamma_1^{\pm} + O(x^2), \quad x \leq 0,$$
(6.20)

where

$$\Gamma_n^{-,+} = -\Psi_n^{-,+} - a_{1,2} \left(\frac{\Lambda_{4+n}^{-,+}}{\kappa_{1,2}^4} - \Lambda_n^{-,+} \right).$$
 (6.21)

For example, by using (5.17c) the stress can be written as

$$\frac{\tau(x)}{b} = -p^{(0)}(x,0) - a\left(\frac{1}{\kappa^4} \frac{d^4}{dx^4} - 1\right) \frac{\partial p^{(0)}}{\partial y}(x,0)
- \sum_{n=0}^{7-q} \Gamma_n^{\pm} \frac{(ix)^n}{n!} + O(x^{7-q} \log|x|), \quad x \leq 0,$$
(6.22)

while the in-surface displacement follows similarly from (2.7).

At this point the maximum value of q in the sum in equation (6.16) can be determined. (6.18 b) implies that the pressure is singular at the join unless q is chosen to satisfy $q \leq 6$. This can also be seen by examining the expansions of the dispersion functions and the Wiener-Hopf split functions at infinity. In doing so, $K^{\pm} = O(1)$ as

 $|\xi| \to \infty$ from Appendices A and B, and $D(\xi) = O(\xi^7)$ at infinity from equation (4.3) so that in order to keep w and $p^{(s)}$ bounded everywhere q is limited to a value of 6.

All that remains is to determine the unknown coefficients $\bar{A}_k, k = 0, 1, \ldots, 6$ in the polynomial A. These are found by application of the various edge conditions at the join located at x = 0. Next we formulate the algebraic system for all the coefficients in this polynomial. We also note that the procedure may be somewhat complicated so that we have provided an outline of the solution method as applied to the simpler case of two joined membranes. This is discussed in Appendix D. For now we continue with two joined curved plates.

(i) Welded join

The first four edge conditions for continuity of the displacement and rotation, w, w, x, and the bending moment and shear force, $Bw_{,xx}$ and $Bw_{,xxx}$, can now be expressed in terms of Λ_n^{\pm} by using equation (5.17) and (6.18):

$$\Lambda_0^+ - \Lambda_0^- = 0, (6.23 a)$$

$$\Lambda_1^+ - \Lambda_1^- = 0, (6.23 b)$$

$$\mu \Lambda_2^+ - \Lambda_2^- = \xi_0^2 (\mu - 1) p_y^{(0)}(0, 0), \tag{6.23} c$$

$$\mu \Lambda_3^+ - \Lambda_3^- = \xi_0^3(\mu - 1)p_y^{(0)}(0, 0), \tag{6.23 d}$$

where

$$\mu = B_2/B_1. (6.24)$$

The remaining two continuity conditions for the in-plane force and in-surface displacement, τ and v, follow from equations (6.22) and (2.7), as

$$\beta \Gamma_0^+ - \Gamma_0^- = -(\beta - 1)p^{(0)}(0, 0) - [\beta \widehat{V}_2(\xi_0) - \widehat{V}_1(\xi_0)]p_u^{(0)}(0, 0), \tag{6.25 a}$$

$$\beta \Gamma_1^+ - \alpha \Gamma_1^- = -\xi_0(\beta - \alpha) p^{(0)}(0, 0) - \xi_0[\beta \widehat{V}_2(\xi_0) - \alpha \widehat{V}_1(\xi_0)] p_{,y}^{(0)}(0, 0), \tag{6.25 b}$$

where

$$\alpha = a_2/a_1, \quad \beta = b_2/b_1.$$
 (6.26)

Equations (6.17), (6.23) and (6.25) constitute a set of seven equations for the seven unknowns \bar{A}_n , $n=0,1,\ldots,6$. An explicit linear system of equations for these unknowns follows from equations (6.19) and (6.21). However, the two kinematic conditions (6.23 a) and (6.23 b) turn out to be trivially satisfied. Thus, as mentioned previously, $\lambda_j^+ = \lambda_j^-$ for j=0–5; therefore, (6.23 a) and (6.23 b) imply, respectively, that $\bar{A}_6 = 0$ and $\bar{A}_5 = 0$. Hence, A is actually fourth order (q=4) and there are, in general, five equations to be satisfied: (6.17), (6.23 c), (6.23 d), (6.25 a) and (6.25 b).

Furthermore, by choosing

$$A(\xi) = A_0 + (\xi - \xi_0) \sum_{n=1}^{4} \tilde{A}_n \xi^{n-1}, \tag{6.27}$$

equation (6.17) is satisfied which then reduces the system to four equations to determine the unknown \tilde{A}_n . These are (6.23 c), (6.23 d), (6.25 a) and (6.25 b), which can

be written, by using equations (6.18) and (6.19), as

$$\sum_{j=1}^{4} \tilde{A}_{j}(\mu \tilde{\lambda}_{1+j}^{+} - \tilde{\lambda}_{1+j}^{-}) = \xi_{0}^{2}(\mu - 1)p_{,y}^{(0)}(0,0) - A_{0}(\mu \lambda_{2}^{+} - \lambda_{2}^{-}), \tag{6.28 a}$$

$$\sum_{j=1}^{4} \tilde{A}_{j}(\mu \tilde{\lambda}_{2+j}^{+} - \tilde{\lambda}_{2+j}^{-}) = \xi_{0}^{3}(\mu - 1)p_{,y}^{(0)}(0,0) - A_{0}(\mu \lambda_{3}^{+} - \lambda_{3}^{-}), \tag{6.28b}$$

and

$$\sum_{j=1}^{4} \tilde{A}_{j} \left\{ \beta \left[\tilde{\psi}_{j-1}^{+} + a_{2} \left(\frac{\tilde{\lambda}_{3+j}^{+}}{\kappa_{2}^{4}} - \tilde{\lambda}_{j-1}^{+} \right) \right] - \left[\tilde{\psi}_{j-1}^{-} + a_{1} \left(\frac{\tilde{\lambda}_{3+j}^{-}}{\kappa_{1}^{4}} - \tilde{\lambda}_{j-1}^{-} \right) \right] \right\} \\
= (\beta - 1)p^{(0)}(0,0) + [\beta \hat{V}_{2}(\xi_{0}) - \hat{V}_{1}(\xi_{0})]p_{,y}^{(0)}(0,0) \\
- A_{0} \left\{ \beta \left[\psi_{0}^{+} + a_{2} \left(\frac{\lambda_{4}^{+}}{\kappa_{2}^{4}} - \lambda_{0}^{+} \right) \right] - \left[\psi_{0}^{-} + a_{1} \left(\frac{\lambda_{4}^{-}}{\kappa_{1}^{4}} - \lambda_{0}^{-} \right) \right] \right\}, \quad (6.29 a) \right\} \\
\sum_{j=1}^{4} \tilde{A}_{j} \left\{ \beta \left[\tilde{\psi}_{j}^{+} + a_{2} \left(\frac{\tilde{\lambda}_{4+j}^{+}}{\kappa_{2}^{4}} - \tilde{\lambda}_{j}^{+} \right) \right] - \left[\tilde{\psi}_{j}^{-} + a_{1} \left(\frac{\tilde{\lambda}_{4+j}^{-}}{\kappa_{1}^{4}} - \tilde{\lambda}_{j}^{-} \right) \right] \right\} \\
= \xi_{0}(\beta - \alpha)p^{(0)}(0,0) + \xi_{0}[\beta \hat{V}_{2}(\xi_{0}) - \alpha \hat{V}_{1}(\xi_{0})]p_{,y}^{(0)}(0,0) \\
- A_{0} \left\{ \beta \left[\psi_{1}^{+} + a_{2} \left(\frac{\lambda_{5}^{+}}{\kappa_{2}^{4}} - \lambda_{1}^{+} \right) \right] - \left[\psi_{1}^{-} + a_{1} \left(\frac{\lambda_{5}^{-}}{\kappa_{1}^{4}} - \lambda_{1}^{-} \right) \right] \right\}, \quad (6.29 b) \right\}$$

where the various combinations of λ_n , ψ_n and $\tilde{\lambda}_n$, $\tilde{\psi}_n$ are given by (B 11) and (B 13), respectively.

(ii) Clamped join

In the instance where the two curved plates are clamped at x=0, then $w, w_{,x}$ and v all vanish at either plate termination. The out-of-plane conditions $(w(\pm 0)=0)$ and $w_{,x}(\pm 0)=0$ then follow as

$$\Lambda_0^+ - \Lambda_0^- = 0, (6.30 a)$$

$$\Lambda_1^+ - \Lambda_1^- = 0, \tag{6.30 b}$$

$$\Lambda_0^+ = p_y^{(0)}(0,0), \tag{6.30c}$$

$$\Lambda_1^+ = \xi_0 p_{,y}^{(0)}(0,0), \tag{6.30 d}$$

and the in-plane conditions $(v(\pm 0) = 0)$ are

$$\Gamma_1^- = -\xi_0[p^{(0)}(0,0) + \hat{V}_1(\xi_0)p_{,y}^{(0)}(0,0)], \tag{6.31a}$$

$$\Gamma_1^+ = -\xi_0[p^{(0)}(0,0) + \widehat{V}_2(\xi_0)p_{,y}^{(0)}(0,0)]. \tag{6.31b}$$

Once again the first two equations of (6.30) are trivially satisfied, reducing q to 4, and (6.17) is also satisfied by choosing the polynomial A to be represented by (6.27), leaving one with the following system of equations to determine the remaining

coefficients of A:

$$\sum_{j=1}^{4} \tilde{A}_{j} \tilde{\lambda}_{j-1}^{+} = p_{,y}^{(0)}(0,0) - A_{0} \lambda_{0}^{+}, \tag{6.32 a}$$

$$\sum_{j=1}^{4} \tilde{A}_j \tilde{\lambda}_j^+ = \xi(\mu - 1) p_{,y}^{(0)}(0,0) - A_0 \lambda_1^+, \tag{6.32b}$$

and, again referring to Appendix B,

$$\sum_{j=1}^{4} \tilde{A}_{j} \left\{ \tilde{\psi}_{j}^{-} + a_{1} \left(\frac{\tilde{\lambda}_{4+j}^{-}}{\kappa_{1}^{4}} - \tilde{\lambda}_{j}^{-} \right) \right\} \\
= \xi_{0} [p^{(0)}(0,0) + \hat{V}_{1}(\xi_{0})p_{,y}^{(0)}(0,0)] - A_{0} \left[\psi_{1}^{-} + a_{1} \left(\frac{\lambda_{5}^{-}}{\kappa_{1}^{4}} - \lambda_{j}^{-} \right) \right], \quad (6.33 \, a) \\
\sum_{j=1}^{4} \tilde{A}_{j} \left\{ \tilde{\psi}_{j}^{+} + a_{2} \left(\frac{\tilde{\lambda}_{4+j}^{+}}{\kappa_{2}^{4}} - \tilde{\lambda}_{j}^{+} \right) \right\} \\
= \xi_{0} [p^{(0)}(0,0) + \hat{V}_{2}(\xi_{0})p_{,y}^{(0)}(0,0)] - A_{0} \left[\psi_{1}^{-} + a_{2} \left(\frac{\lambda_{5}^{-}}{\kappa_{2}^{4}} - \lambda_{1}^{-} \right) \right]. \quad (6.33 \, b) \\
= \xi_{0} [p^{(0)}(0,0) + \hat{V}_{2}(\xi_{0})p_{,y}^{(0)}(0,0)] - A_{0} \left[\psi_{1}^{-} + a_{2} \left(\frac{\lambda_{5}^{-}}{\kappa_{2}^{4}} - \lambda_{1}^{-} \right) \right]. \quad (6.33 \, b) \\
= \xi_{0} [p^{(0)}(0,0) + \hat{V}_{2}(\xi_{0})p_{,y}^{(0)}(0,0)] - A_{0} \left[\psi_{1}^{-} + a_{2} \left(\frac{\lambda_{5}^{-}}{\kappa_{2}^{4}} - \lambda_{1}^{-} \right) \right]. \quad (6.33 \, b) \\
= \xi_{0} [p^{(0)}(0,0) + \hat{V}_{2}(\xi_{0})p_{,y}^{(0)}(0,0)] - A_{0} \left[\psi_{1}^{-} + a_{2} \left(\frac{\lambda_{5}^{-}}{\kappa_{2}^{4}} - \lambda_{1}^{-} \right) \right]. \quad (6.33 \, b) \\
= \xi_{0} [p^{(0)}(0,0) + \hat{V}_{2}(\xi_{0})p_{,y}^{(0)}(0,0)] - A_{0} \left[\psi_{1}^{-} + a_{2} \left(\frac{\lambda_{5}^{-}}{\kappa_{2}^{4}} - \lambda_{1}^{-} \right) \right]. \quad (6.33 \, b) \\
= \xi_{0} [p^{(0)}(0,0) + \hat{V}_{2}(\xi_{0})p_{,y}^{(0)}(0,0)] - A_{0} \left[\psi_{1}^{-} + a_{2} \left(\frac{\lambda_{5}^{-}}{\kappa_{2}^{4}} - \lambda_{1}^{-} \right) \right]. \quad (6.33 \, b) \\
= \xi_{0} [p^{(0)}(0,0) + \hat{V}_{2}(\xi_{0})p_{,y}^{(0)}(0,0)] - A_{0} \left[\psi_{1}^{-} + a_{2} \left(\frac{\lambda_{5}^{-}}{\kappa_{2}^{4}} - \lambda_{1}^{-} \right) \right]. \quad (6.33 \, b) \\
= \xi_{0} [p^{(0)}(0,0) + \hat{V}_{2}(\xi_{0})p_{,y}^{(0)}(0,0)] - A_{0} \left[\psi_{1}^{-} + a_{2} \left(\frac{\lambda_{5}^{-}}{\kappa_{2}^{4}} - \lambda_{1}^{-} \right) \right]. \quad (6.33 \, b) \\
= \xi_{0} [p^{(0)}(0,0) + \hat{V}_{2}(\xi_{0})p_{,y}^{(0)}(0,0)] - A_{0} \left[\psi_{1}^{-} + a_{2} \left(\frac{\lambda_{5}^{-}}{\kappa_{2}^{4}} - \lambda_{1}^{-} \right) \right]. \quad (6.33 \, b) \\
= \xi_{0} [p^{(0)}(0,0) + \hat{V}_{2}(\xi_{0})p_{,y}^{(0)}(0,0)] - A_{0} \left[\psi_{1}^{-} + a_{2} \left(\frac{\lambda_{5}^{-}}{\kappa_{2}^{4}} - \lambda_{1}^{-} \right) \right]$$

7. Limiting cases

Several interesting and physically important special cases deserve discussion. We consider in succession the following situations: (a) two curved plates with identical mechanical properties; (b) one flat plate; (c) the FPL* case; and (d) both plates flat.

(a) Identical plates: change in curvature

The mechanical properties of the plates are the same, $a_1 = a_2$, $k_1 = k_2$, $\kappa_1 = \kappa_2$, but $b_1 \neq b_2$. The main simplification is that the polynomial P^* reduces to a quadratic, with roots $\pm \zeta_1 = \pm k_1$. Hence, the reflection coefficients R_1 and R_2 coincide at this wave number, and the diffraction problem for the pressure becomes trivial $(p^{(s)} = 0)$ if $\xi_0 = \pm k_1$.

(b) One flat plate

The general set of edge conditions needs to be amended when one or both plates has zero curvature. Referring to equations (2.1) and (5.17 c) it should be clear that τ_0 should vanish on the flat side of the junction. To be specific, if we let plate 1 be flat, then it follows from (6.13) that $\tau_0(x)$ for x < 0 depends upon

$$\tilde{\tau}_{0}(\xi) = -\frac{D_{1}(\xi)}{U_{1}(\xi)}\tilde{p}_{0}(\xi)
= -G(\xi_{0})\frac{K^{-}(\xi)}{U_{1}(\xi)}
= -\frac{G(\xi_{0})K^{-}(-k_{1})}{2k_{1}(k_{1}+\xi)} + \frac{G(\xi_{0})}{k_{1}+\xi} \left[\frac{K^{-}(-k_{1})}{2k_{1}} - \frac{K^{-}(\xi)}{k_{1}-\xi} \right].$$
(7.1)

The scattered stress for x < 0 therefore depends upon the first term on the right-hand side, because the other is analytic in \mathcal{H}^- . Noting that $|b_1| \to \infty$, and $p^{(0)}$ for x < 0 in equation (5.17 a) implies that in order for the stress at the junction to be finite, we must have

$$A(-k_1) = 0. (7.2)$$

This condition replaces condition (6.25 a), and holds whatever the incident wave type may be: acoustic, flexural or longitudinal (FPL).

The actual value of the scattered (total minus incident) stress at the junction is then given by evaluating (5.17c) on the curved side (x = 0+), yielding

$$\tau^{(s)}(0) = -\tau^{(0)}(0) - b_2 \{ p^{(0)}(0,0) + \widehat{V}_2(\xi_0) p_{,y}^{(0)}(0,0) + \Gamma_0^+ \}.$$
 (7.3)

Note that $\tau^{(0)} = 0$ unless the incident excitation is from a FPL wave, in which case it is given by equation (5.3). In either case, the scattered stress on plate 1 must be of the form (cf. equation (2.6))

$$\tau^{(s)}(x) = \tau^{(s)}(0)e^{-ik_1x}, \quad x < 0,$$
 (7.4)

i.e. the value of the diffracted FPL wave is determined by the stress at the junction. If the incidence is acoustic or flexural, we have the general result: the amplitude of the diffracted longitudinal stress wave on a flat plate is precisely the value of the stress at the junction.

Finally, the v-condition at x = 0 for a welded junction is given by (5.17 c), using the value from (7.4) for the flat side:

$$\Gamma_1^+ = \frac{\mathrm{i}\alpha}{b_2} [\tau_{,x}^{(0)}(0) - \mathrm{i}k_1\tau^{(s)}(0)] - \xi_0[p^{(0)}(0,0) + \widehat{V}_2(\xi_0)p_{,y}^{(0)}(0,0)]. \tag{7.5}$$

After substituting the junction stress and its derivative given by equations (7.3) and (7.4), one arrives at

$$\Gamma_1^+ + \alpha k_1 \Gamma_0^+ = \frac{i\alpha}{b_2} [\tau_{,x}^{(0)}(0) + ik_1 \tau^{(0)}(0)] - (\xi_0 + \alpha k_1) [p^{(0)}(0,0) + \widehat{V}_2(\xi_0) p_{,y}^{(0)}(0,0)].$$
 (7.6)

The full set of seven equations required to determine A are (6.17), (6.23), (7.2) and (7.6). We note that equations (6.23 a) and (6.23 b) are identically satisfied so that the order of A is reduced to four. Further simplifications are obtained by choosing the polynomial A in the following manner:

$$A(\xi) = \frac{\xi + k_1}{\xi_0 + k_1} \left[A_0 + (\xi - \xi_0) \sum_{j=1}^{3} \tilde{A}_j \xi^{j-1} \right], \tag{7.7}$$

which leaves us with three remaining conditions to determine the unknown \tilde{A}_j with j=1,2,3. They are $(6.23\,c),\,(6.23\,d)$ and (7.6). If the joint between the two plates is clamped, then the remaining three conditions are $(6.30\,c),\,(6.30\,d),\,$ and $(6.31\,b),\,$ which applies only for acoustic or flexural incidence. For longitudinal wave incidence $(5.3),\,$ the solution for a clamped joint is trivial with the reflected stress being equal in amplitude to the incident stress, but now as an outgoing wave.

In this special case plate 1 is flat, the incident excitation is a longitudinal wave propagating towards the junction on this plate, and the longitudinal wave numbers are identical on both plates, i.e. $k_2 = k_1$. Then, as noted in § 5, A_0 vanishes, but a nontrivial solution satisfying this condition can be found. Referring to equations (5.14) and (5.15) it is clear that $A(\xi)$ also vanishes at $\xi = \xi_0$, and so must be of the form $A(\xi) = (\xi - \xi_0)A^*(\xi)$. Therefore, the general solution is

$$\tilde{p}(\xi) = A^*(\xi) \frac{G(\xi_0)}{G(\xi)},$$
(7.8)

which satisfies the dual condition of equation (5.6) with $A_0 = 0$, again as long as $A^*(\xi)$ is a polynomial, chosen accordingly. In summary, this case is really no different from that of a a flat plate with $k_1 \neq k_2$, except that $A_0 = 0$. However, the general solution of equations (5.14) and (5.15) still works with

$$A^*(\xi) = \frac{\xi + k_1}{\xi_0 + k_1} \sum_{j=1}^3 \tilde{A}_j \xi^{j-1}, \tag{7.9}$$

using equations (6.23 c), (6.23 d) and (7.6) to determine the unknown coefficients.

(d) Two flat plates

When both plates have zero curvature the same argument which led to the condition (7.2) implies the analogous argument

$$A(k_2) = 0. (7.10)$$

The full set of equations are therefore (6.17), (6.23), (7.2) and (7.10). The final two imply that

$$A(\xi) = \left(\frac{\xi + k_1}{\xi_0 + k_1}\right) \left(\frac{\xi - k_2}{\xi_0 - k_2}\right) A^*(\xi). \tag{7.11}$$

Using previous arguments it can easily be seen that A^* is now a second-order polynomial which we choose as

$$A^*(\xi) = A_0 + (\xi - \xi_0)(\tilde{A}_1 + \tilde{A}_2 \xi), \tag{7.12}$$

subject to the conditions (6.23 c) and (6.23 d).

After some reconsideration of the equations, and of the physics, particularly the decoupling of the longitudinal motion, it is clear that the solution depends only upon the flexural plate equation. This is obtained by setting U=1 and $V=\widehat{V}$ (cf. (4.5)) in the definition of the dispersion functions, which then gives

$$P(\xi) = 1 - a^2 \left(\frac{\xi^{10}}{\kappa^8} - \frac{k_{\rm f}^2 \xi^8}{\kappa^8} - \frac{2\xi^6}{\kappa^4} + 2\frac{k_{\rm f}^2}{\kappa^4} \xi^4 + \xi^2 - k_{\rm f}^2 \right), \tag{7.13}$$

so that N = 10. The polynomial P^* is fourth order $(N^* = 4)$, P_0^* is the same as in (6.6), so the roots are explicitly given by

$$\zeta_n^4 = (a_2 - a_1) \left(\frac{a_2}{\kappa_2^4} - \frac{a_1}{\kappa_1^4} \right)^{-1} = \kappa_1^4 \left(\frac{\alpha - 1}{\mu - 1} \right). \tag{7.14}$$

Further simplifications arise in the course of the derivation, the most significant of which are that A^* replaces A, and that the coefficients in Appendix A take on simpler forms.

The remaining two conditions (6.23 c) and (6.23 d) can be reduced to give

$$\begin{bmatrix}
(\mu - 1)(\lambda_3^{\pm} - \xi_0 \lambda_2^{\pm}) & \mu(\lambda_4^{+} - \xi_0 \lambda_3^{\pm}) - (\lambda_4^{-} - \xi_0 \lambda_3^{\pm}) \\
\mu(\lambda_4^{+} - \xi_0 \lambda_3^{\pm}) - (\lambda_4^{-} - \xi_0 \lambda_3^{\pm}) & \mu(\lambda_5^{+} - \xi_0 \lambda_4^{+}) - (\lambda_5^{-} - \xi_0 \lambda_4^{-}) \end{bmatrix} \begin{bmatrix} \tilde{A}_1 \\ \tilde{A}_2 \end{bmatrix} \\
= (\mu - 1) \begin{bmatrix} \xi_0^2 p_{,y}^{(0)}(0, 0) - A_0 \lambda_2^{\pm} \\ \xi_0^3 p_{,y}^{(0)}(0, 0) - A_0 \lambda_3^{\pm} \end{bmatrix}, (7.15)$$

where $\lambda_j^+ = \lambda_j^-$ for j = 0, 1, 2 and 3, only. The matrix elements can be reduced by first noting that, from (6.9), we have K = 1 at the two roots $\zeta_{\rm m}$, m = 1, 2, in \mathcal{H}^+ , and hence, $K^-(\zeta_{\rm m}) = K^+(\zeta_{\rm m})$. Define the phase of the split functions at the roots by

$$K^{+}(\zeta_{\rm m}) = e^{\nu_{\rm m}}.$$
 (7.16)

Then, by using (B 11) and the fact that $K_{\infty}^{+} = \sqrt{\mu}$, we have

$$\lambda_3^{\pm} - \xi_0 \lambda_2^{\pm} = \frac{G(\xi_0)}{2P_0^*} \sum_{m=1}^2 \frac{\sinh \nu_{\rm m}}{\zeta_{\rm m}},\tag{7.17a}$$

$$\lambda_4^{\pm} - \xi_0 \lambda_3^{\pm} = \frac{G(\xi_0)}{2P_0^*} \left\{ \sum_{m=1}^2 \cosh \nu_m - 2(\sqrt{\mu})^{\mp 1} \right\}, \tag{7.17b}$$

$$\lambda_5^{\pm} - \xi_0 \lambda_4^{\pm} = \frac{G(\xi_0)}{2P_0^*} \left\{ \sum_{m=1}^2 \zeta_m \sinh \nu_m - 2\beta_1^{\mp} (\sqrt{\mu})^{\mp 1} \right\}.$$
 (7.17 c)

where $\beta_1^+ = \beta_1^-$ (see Appendix A) and the terms u_{1m}^+ have been simplified by using (6.8) and (7.14). Now using (7.17) for the matrix, and (B 14) and (B 11) for $p_{,y}^{(0)}(0,0)$ and λ_2^{\pm} , equation (7.15) becomes exactly

$$\frac{G(\xi_0)}{2P_0^*} \sum_{m=1}^2 \begin{bmatrix} (1/\zeta_{\rm m}) \sinh \nu_{\rm m} & \cosh \nu_{\rm m} \\ \cosh \nu_{\rm m} & \zeta_{\rm m} \sinh \nu_{\rm m} \end{bmatrix} \begin{bmatrix} \tilde{A}_1 \\ \tilde{A}_2 \end{bmatrix}
= -A_0 \frac{G(\xi_0)}{2P_0^*} \sum_{m=1}^2 \frac{1}{\zeta_{\rm m}^2 - \xi_0^2} \begin{bmatrix} \cosh \nu_{\rm m} + (\xi_0/\zeta_{\rm m}) \sinh \nu_{\rm m} \\ \xi_0 \cosh \nu_{\rm m} + \zeta_{\rm m} \sinh \nu_{\rm m} \end{bmatrix}. (7.18)$$

Finally, using $\zeta_1^2 + \zeta_2^2 = 0$, see equation (7.14), and solving the matrix system, (7.18) yields

$$A^{*}(\xi) = \frac{A_{0}}{\zeta_{1}^{4} - \xi_{0}^{4}} \left\{ \zeta_{1}^{4} - \xi^{2} \xi_{0}^{2} - \frac{(\xi - \xi_{0})}{1 + \cosh \nu_{1} \cosh \nu_{2}} [(\xi - \xi_{0}) \zeta_{1} \zeta_{2} \sinh \nu_{1} \sinh \nu_{2} + (\xi \xi_{0} + \zeta_{1}^{2}) \zeta_{1} \sinh \nu_{1} \cosh \nu_{2} + (\xi \xi_{0} + \zeta_{2}^{2}) \zeta_{2} \sinh \nu_{2} \cosh \nu_{1}] \right\}.$$
(7.19)

This clearly satisfies the reciprocity condition (5.29). For the case of a clamped join, the junction conditions change to those given by (6.16), (6.30 c) and (6.30 d). Repeating the previous analysis using clamped joint conditions, the polynomial A is

found to be similar to (7.19), the only difference being that the $1 + \cosh \nu_1 \cosh \nu_2$ term is replaced by $1 - \cosh \nu_1 \cosh \nu_2$.

At this point we refer the reader to the paper by Norris & Wickham (1995) for further discussion on two flat plates, which includes both light and heavy fluid-loading limits.

8. Numerical results

The numerical results reported here are for pairs of plates that are identical in every regard except thickness and curvature. Therefore, α of equation (6.26) is just the ratio of thicknesses, and the flat plate flexural wave numbers are simply related by $\kappa_2 = \kappa_1/\sqrt{\alpha}$. The conventional dimensionless fluid-loading parameter $\varepsilon = (k_{\rm f}h)/(ka)/\sqrt{12}$ (Crighton & Innes 1984) is identical for both plates. We consider steel plates loaded by water ($\varepsilon = 0.134$) with the join of the plates either welded or clamped. Based upon the computations reported by Norris & Wickham (1995), who compared steel/water and aluminium/water ($\varepsilon = 0.4$) flat plate systems, we do not expect the results to depend strongly upon ε for metallic structures in water.

The present results extend the flat plate calculations of Brazier-Smith (1987) and Norris & Wickham (1995) by introducing different radii of curvature for each plate in addition to the contrast provided by a discontinuity in plate thickness. We consider a thickness change of 100% or $\alpha=2$ with plate 1 being 0.0254 m thick. As a representative example, the radii of curvatures were chosen to be 0.5 m for shell 1 and 1 m for shell 2. The null, ring and coincidence frequencies are 47, 1730 and 8916 Hz for shell 1 and 94, 865 and 4493 Hz for shell 2. Equation (3.1) then implies that the frequency must be greater than 238 Hz. The present theory is not valid below this frequency. We find that the trends in the results are qualitatively similar for typical choices of radii of curvature, with the main effects depending upon the increase or decrease of the ring frequency.

The results in figures 3–7 are presented as a function of the non-dimensional frequency Ω , which is based upon the coincidence frequency (the frequency at which $k_f = \kappa$) of plate 1:

$$\Omega = k_{\rm f}^2 / \kappa_1^2. \tag{8.1}$$

Thus, the coincidence frequency of plate 1 occurs at $\Omega=1$ and for plate 2 at $\Omega=0.5$. The curved plates have identical ring frequencies at $\Omega=0.1925$ for the chosen parameters, and hence we only plot results for $\Omega \geqslant 0.2$.

The diffraction coefficients of structural waves on a pair of curved plates generated by an incident subsonic flexural wave are plotted in figure 3. These curves display the pressure amplitude for unit incident pressure p_0 . It is observed that subsonic flexural transmission is strongest for a welded join whereas a clamped join generates a larger reflected longitudinal wave. The peaks in the subsonic flexural coefficients occur at approximately the coincidence frequency of each plate. This is the frequency at which the fluid wave number matches the subsonic flexural wave number of the curved plate (cf. Photiadis 1995; Rebinsky & Norris 1995b). It is interesting to note that the diffracted pressure amplitudes of the longitudinal waves are of the same order as those of the subsonic flexural waves.

The redistribution of structural wave energy is shown in figures 4–6 for an incident subsonic flexural wave. The partition of diffracted energy on two joined flat plates

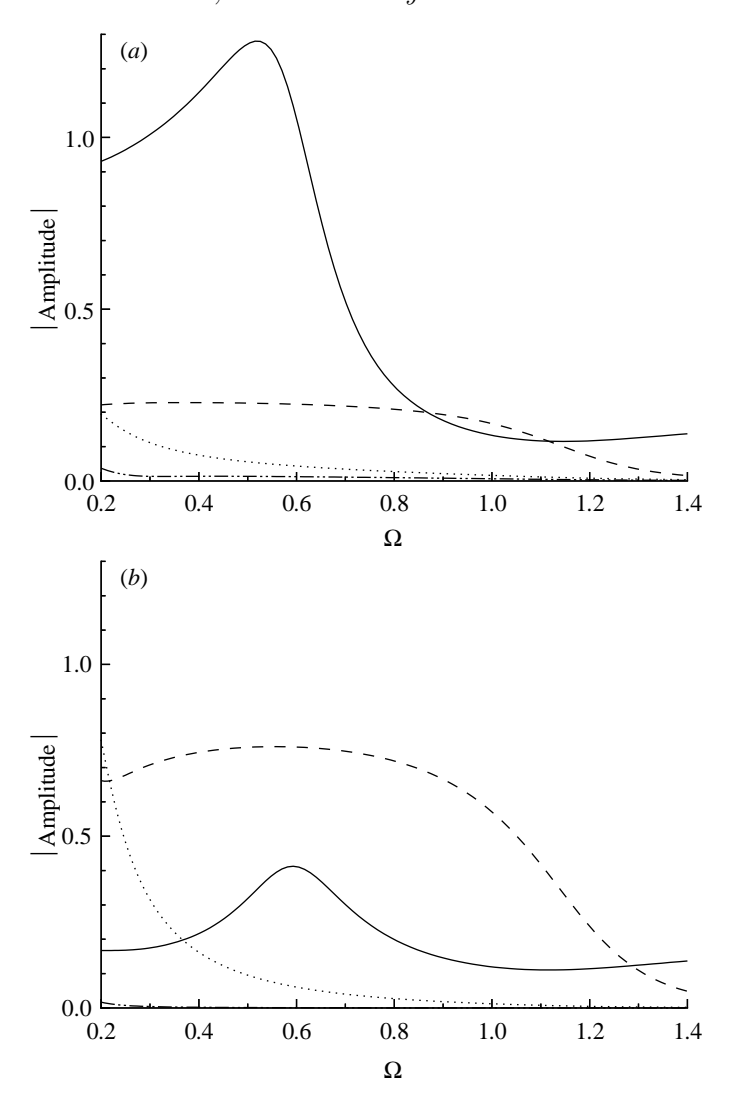


Figure 3. Amplitudes of the reflected and transmitted structural waves generated by the (a) welded and (b) clamped joining of two curved plates: - - - - -, reflected subsonic flexural; —, transmitted subsonic flexural; ····, reflected longitudinal; -··-, transmitted longitudinal.

(Norris & Wickham 1995) is shown for comparison. In general most of the energy flow from the junction is contained in the diffracted subsonic flexural waves at lower frequencies (figure 4) and in acoustic diffraction at higher frequencies (figure 5). However, the details vary considerably for the welded and clamped plates, which are discussed separately next.

The energy partition for a welded join is shown in figures 4a, 5a and 6a. It is evident that the transmitted flexural energy is influenced strongly by the curvature contrast, and it decreases for large contrast (large β). The reflected flexural power is less sensitive to the curvature contrast. There is also a significant amount of reflected and transmitted longitudinal energy generated at the discontinuity. For the configuration

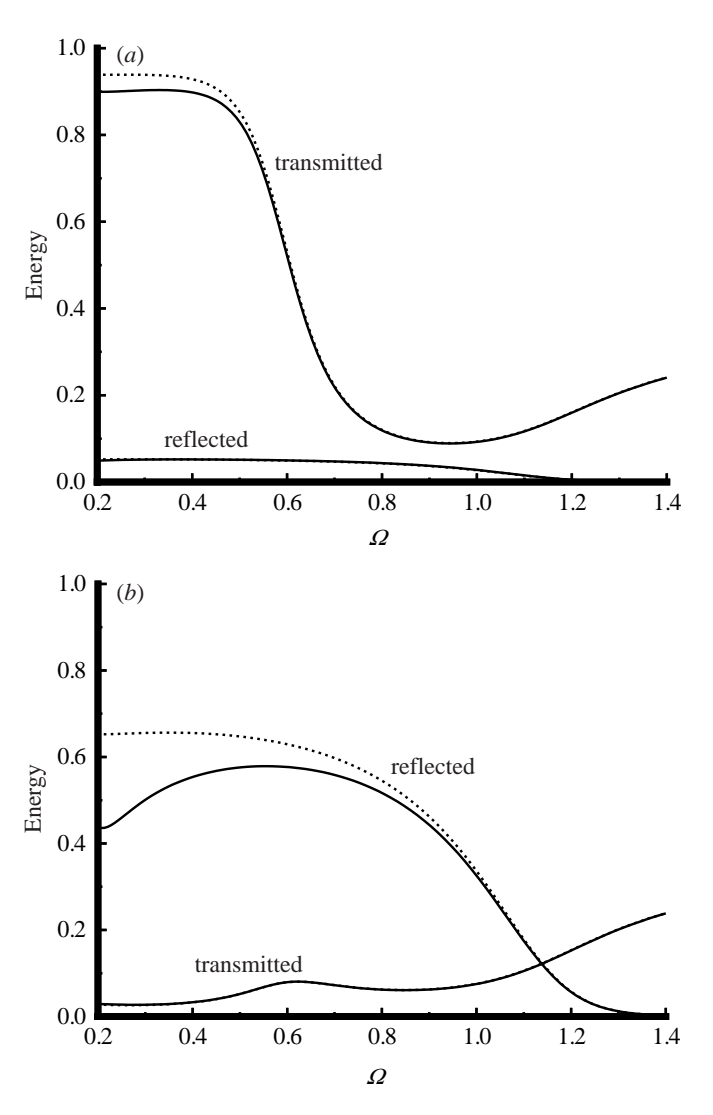


Figure 4. Partition of reflected and transmitted flexural energy for flat plate and curved plate systems where the junction is (a) welded and (b) clamped: \cdots , both flat plates; —, both curved plates.

considered in the figures, each longitudinal wave contains approximately 5% of the total energy over a wide range of frequencies.

Turning to the clamped join, figures 4b, 5b and 6b, we see that an increase of the curvature contrast, β , diminishes both the reflected flexural energy and the acoustical diffraction near the ring frequency. The reflected longitudinal energy is significant for $\Omega < 1$. The increase in the amount of reflected longitudinal energy at the expense of the other wave types may be explained by the enhanced coupling between normal and in-plane motion that occurs as the plates are curved. It is not surprising that the transmitted longitudinal energy is negligibly small. This is because the only means

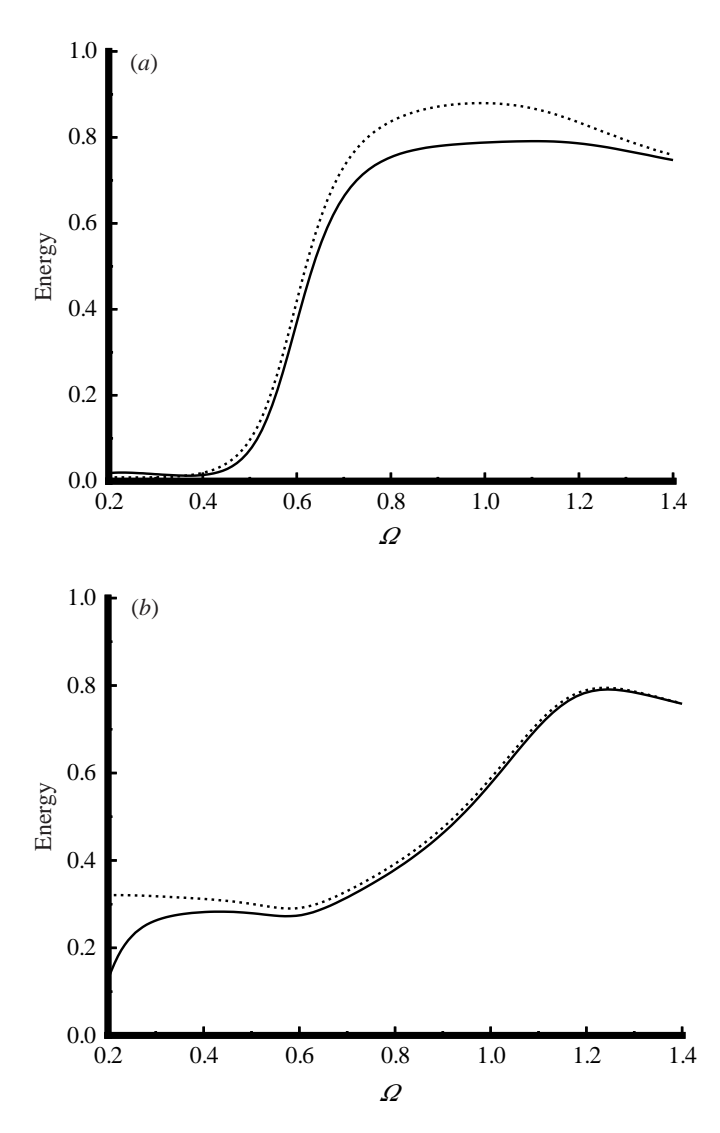


Figure 5. Acoustic radiated energy for flat plate and curved plate systems where the junction is (a) welded and (b) clamped: \cdots , both plates flat; \longrightarrow , both curved plates.

of interaction between the incident structural wave and plate 2 is through the fluid, which couples strongly to normal motion but very weakly to in-plane motion.

Longitudinal wave incidence from a flat plate onto a curved plate with radius of curvature of 1 m is considered in figure 7. We find that most of the energy is converted into diffracted longitudinal waves. At high frequencies, the curved plate appears flat and the longitudinal energies approach their in vacuo values of $\frac{1}{9}$ reflected and $\frac{8}{9}$ transmitted for $\alpha=2$. If the joint is clamped instead of being welded, the trivial result of total reflection is obtained.

It is of some interest to study the directivity of the acoustic diffraction pattern generated by a subsonic flexural wave striking the join. We find that the directivity is

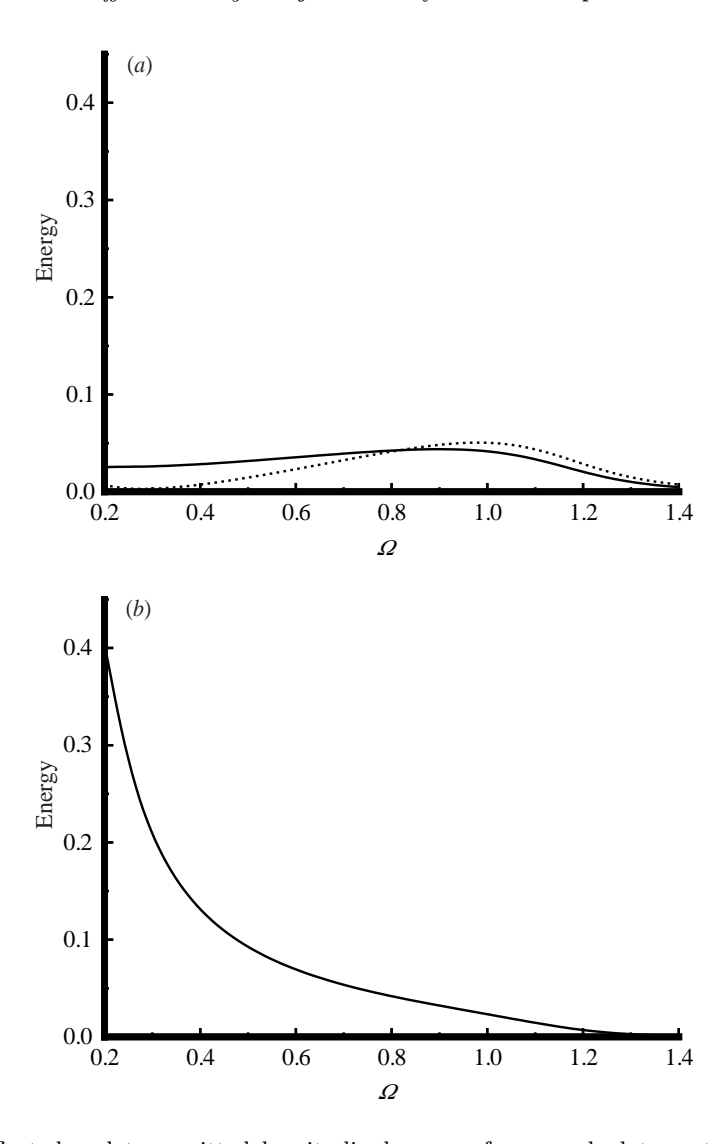


Figure 6. Reflected and transmitted longitudinal energy for curved plate systems where the junction is (a) welded and (b) clamped: —, reflected longitudinal energy; \cdots , transmitted longitudinal energy. Note that the amount of transmitted longitudinal energy for a clamped junction is negligibly small.

dramatically dependent upon the type of junction, the frequency regime and the curvature of the plates. Brazier-Smith (1987) and Norris & Wickham (1995) examined the acoustic diffraction for different edge conditions over a broad range of frequencies. We therefore focus here on the influence of curvature. Figures 8 and 9 show radiation patterns for $\Omega=0.25,\,0.75$ and 1.25 for both welded and clamped steel plates in water. The total radiated power is small at low frequencies, and the directivity is similar to that of a dipole placed at the plate junction with its axis perpendicular to the tangent line. However, the radiated acoustic field develops intense beams at higher frequencies. The beam directions correlate well with the emergence of leaky

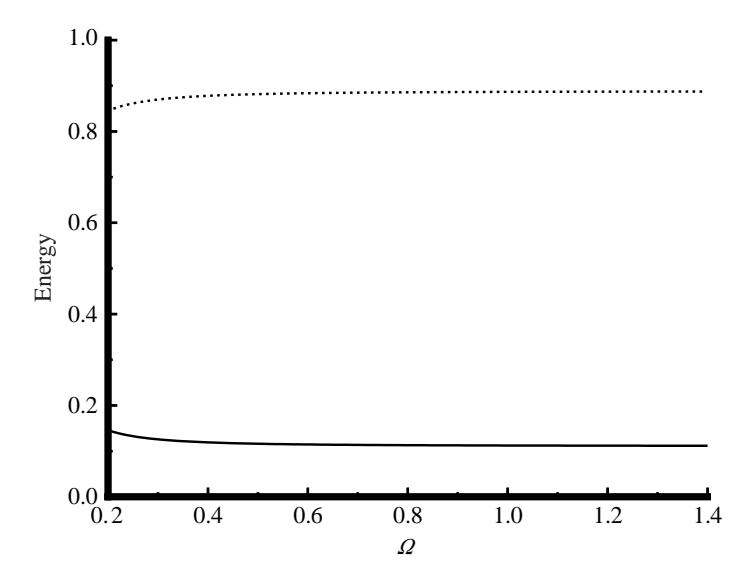


Figure 7. Reflected and transmitted longitudinal wave energy for FPL* incidence on a flat plate welded to a curved plate: ——, reflected longitudinal energy; \cdots , transmitted longitudinal energy.

longitudinal waves that couple to the fluid only when the plates possess curvature. The sharp peaks in the directivity occur at the critical angle for a longitudinal wave, which is approximately 15° for steel and water. When the wave is incident from a flat plate the directivity shows only one sharp beam in the forward direction, corresponding to a leaky wave on the curved plate along x > 0. Two sharp peaks can be seen when both plates are curved, with one in the forward direction and the other in the backward direction (see figures 8 and 9). These beams are strongest when the joint is welded.

Finally, figure 10 shows the acoustic radiation pattern generated by longitudinal wave (FPL*) incidence from a flat plate which strikes the welded joint with a curved plate. We note that the total radiated power is small, although intense beams are present once again at the longitudinal wave critical angle.

9. Conclusions

We have outlined a relatively simple, straightforward method for characterizing acoustic or structural wave interaction with the junction of two curved plates which are unilaterally fluid loaded. The main results are summarized by equations (5.1) and (5.2) for the total response, equation (5.7) for the incident wave field and equations (5.5), (5.15) and (5.16) for the scattered wave field. The Wiener–Hopf split function K^+ is derived in Appendix A in a semi-analytic form which allows for easy computation. The scattered response depends upon a polynomial function A which requires at most a 4×4 linear system of equations to be solved for either welded or clamped plate edges. With these formulae, acoustic–structural wave interactions at junctions between plate segments whether curved or flat can be numerically evaluated over a wide frequency range. Energy flux relations have also been derived for the structural waves in fluid-loaded curved plates. We have illustrated some typical

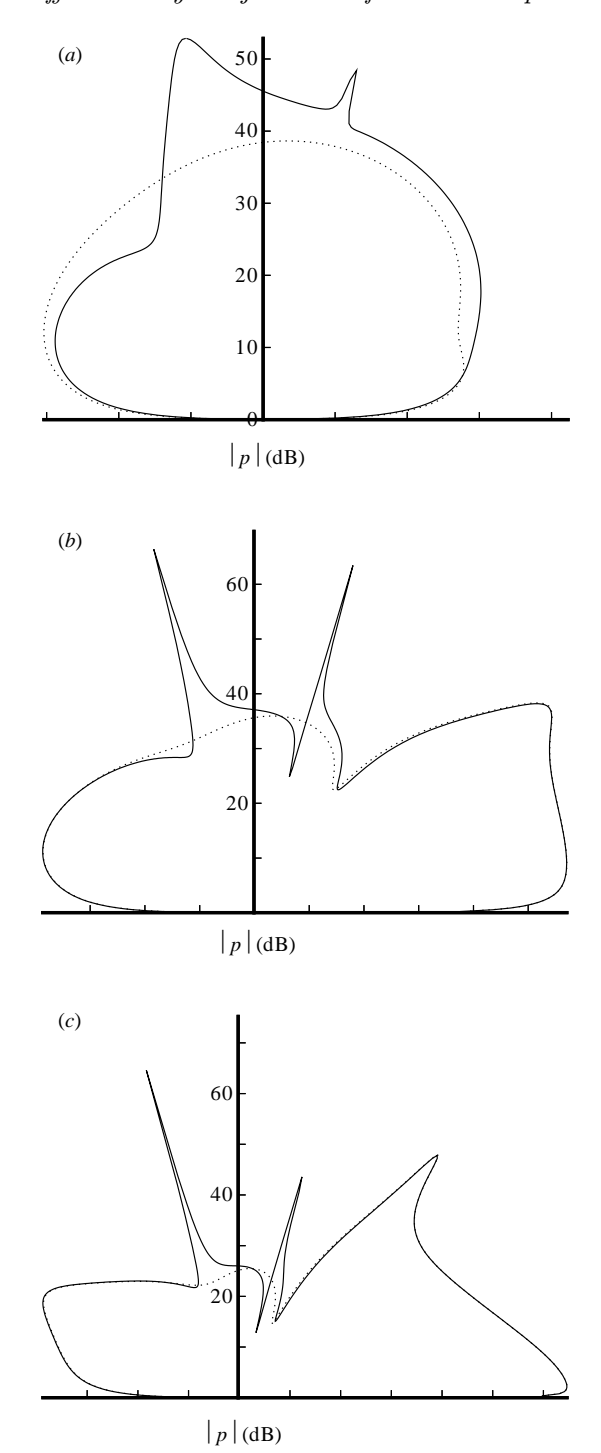


Figure 8. Polar plots of the scattered acoustic pressure amplitude generated at a welded junction of two steel plates loaded by water. The non-dimensional frequencies Ω are (a) 0.25, (b) 0.75 and (c) 1.25: \cdots , both flat plates; —, both curved plates.

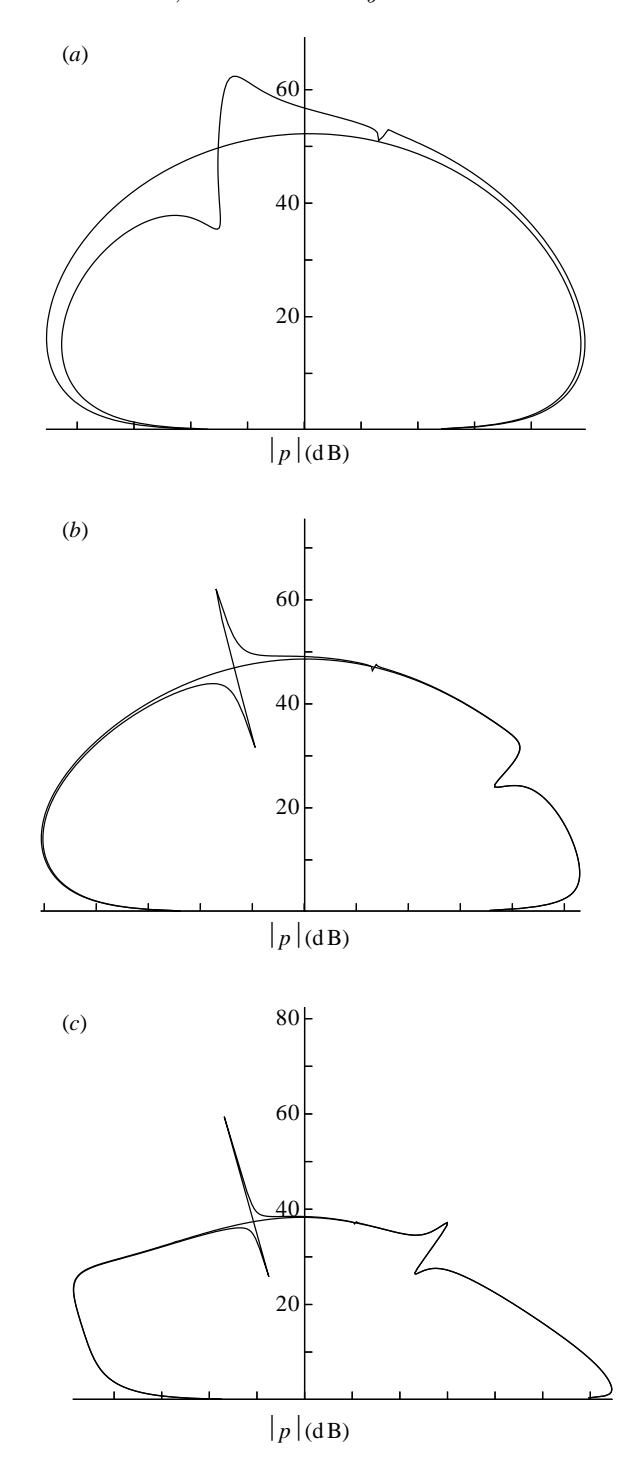


Figure 9. Polar plots of the scattered acoustic pressure amplitude generated at a clamped junction of two steel plates loaded by water. The non-dimensional frequencies Ω are (a) 0.25, (b) 0.75 and (c) 1.25: \cdots , both flat plates; —, both curved plates.

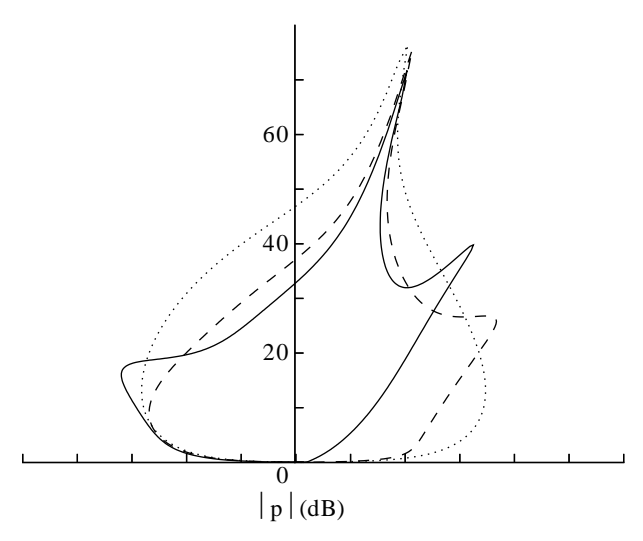


Figure 10. Polar plots of the scattered acoustic pressure amplitude generated at a welded junction of a flat plate with a curved one due to the interaction of a longitudinal wave (FPL*) with the joint: \cdots , $\Omega = 0.25$; ----, $\Omega = 0.75$; ----, $\Omega = 0.25$.

numerical results for various wave interactions by presenting diffraction coefficients and energy distributions.

A.N.N. and D.A.R. were supported by the US Office of Naval Research.

Appendix A. Factorization of the dispersion functions

(a) Preliminary results and definitions

The functions $K^+(\xi)$ and $K^-(\xi)$ defined in equation (5.12) are evaluated here. In general, we can consider any pair of dispersion functions $D_1(\xi)$ and $D_2(\xi)$ that are of the form (4.3) with $U_1(\xi)$ and $V_1(\xi)$ the same order as $U_2(\xi)$ and $V_2(\xi)$, respectively. The fact that D_1 and D_2 are even functions of ξ implies the symmetry property

$$K^{-}(-\xi) = 1/K^{+}(\xi),$$
 (A1)

and therefore

$$K^{+}(0) = \sqrt{D_2(0)/D_1(0)}.$$
 (A 2)

It follows from its definition in (5.16) and from (A1) that the value of $G(\xi)$ is unaltered under the double interchange $1 \leftrightarrow 2$ followed by $\xi \leftrightarrow -\xi$. This symmetry property is apparent in the context of the diffraction problem—it amounts to a mirror symmetry or parity of the system. It is clear from the general solution in equation (5.15) that this function $G(\xi)$ is of fundamental importance.

Define $P(\xi)$ by

$$P(\xi) = D(\xi)\widetilde{D}(\xi) = U^{2}(\xi) + (k_{\rm f}^{2} - \xi^{2})V^{2}(\xi).$$
 (A 3)

Hence, P is a polynomial in ξ^2 , with roots $\xi = \pm \xi_n$, $n = 1, 2, \dots, \frac{1}{2}N$, where N = 14 for the problem as stated. With no loss in generality, we let $\text{Im } \xi_n > 0$. Associated

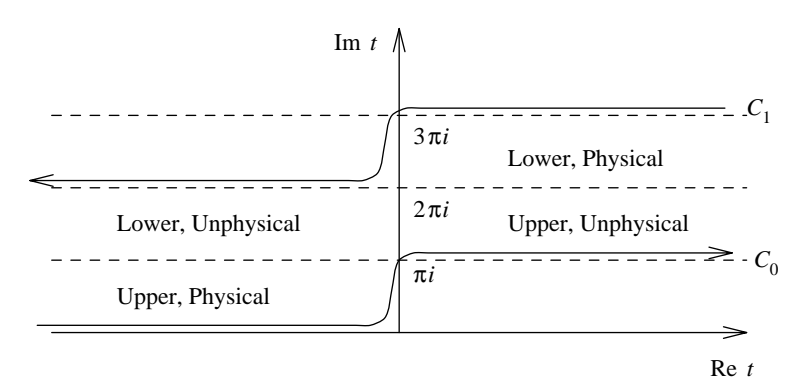


Figure 11. A map of the complex t-plane near the contours C_0 and C_1 . The four quadrants indicated are the images of the corresponding regions in the original complex ξ -plane, where $\xi = -k_{\rm f} \cosh t$. Thus, $\gamma = -k_{\rm f} \sinh t$ has real part positive (negative) in the physical (unphysical) quadrants. Unphysical roots of this equation are all mapped into the unphysical quadrants.

split functions P^+ and P^- are defined by

$$P(\xi) = P^{+}(\xi)P^{-}(\xi),$$
 (A4)

and the constraint

$$P^{-}(-\xi) = P^{+}(\xi). \tag{A 5}$$

Hence,

$$P^{\pm}(\xi) = \frac{a}{\kappa^4} \prod_{n=1}^{N/2} (\xi_n \pm \xi).$$
 (A 6)

Note that the dispersion function can be expressed in terms of P and the reflection coefficient:

$$D(\xi) = R^{-1/2}(\xi)P^{1/2}(\xi). \tag{A 7}$$

We first consider the analytic factorization of the function

$$L(\xi) = R_2(\xi)/R_1(\xi) = L^-(\xi)/L^+(\xi),$$
 (A8)

where $L^{\pm}(\xi)$ are analytic \mathcal{H}^{\pm} , respectively, and they satisfy the same reflection symmetry as K^{\pm} , i.e. $L^{-}(-\xi) = 1/L^{+}(\xi)$. The desired functions then follow from equations (5.12), (A 4), (A 7) and (A 8); for example,

$$K^{+}(\xi) = \left[\frac{P_2^{+}(\xi)}{P_1^{+}(\xi)}L^{+}(\xi)\right]^{1/2}.$$
 (A9)

(b) Analytic splitting

It can be shown by standard means (Noble 1958) that

$$(\log L^{\pm})'(\xi) = -\frac{1}{2\pi i} \int_{-\infty}^{\infty} \frac{[\log L(s)]'}{s - \xi} ds, \tag{A 10}$$

where $f'(s) \equiv df(s)/ds$, and the L^+ contour goes under ξ , the L^- over, for real ξ . Now change integration variables according to the conformal transformation $s = -k_f \cosh t$, $\gamma(s) = -k_f \sinh t$, and focusing on the function L^+ , we have

$$(\log L^{+})'(\xi) = -\frac{1}{2\pi i} \int_{C_0} [\log L(-k_{\rm f} \cosh t)]' \frac{\sinh t \,dt}{\cosh t - \cosh u}, \tag{A 11}$$

where $\xi = -k_{\rm f} \cosh u$, and the contour C_0 runs from $t = -\infty + {\rm i} b$ to $t = \infty + {\rm i} \pi + {\rm i} b$ (see figure 11). The pole associated with real-valued ξ lies slightly above C_0 . The integrand in (A 11) is periodic with period $2\pi {\rm i}$, implying that the contour C_0 could be equally well replaced by any contour C_n , $n = \pm 1, \pm 2, \ldots$, obtained by shifting C_0 by $n2\pi {\rm i}$. Let C be the closed contour formed by combining C_0 , C_1 and vertical contours of length 2π joining the ends of C_0 and C_1 at $\pm \infty$. Let g(t) denote the integrand of (A 11), then the integral of g(t) around the closed contour C is identically zero. However, consider the integral of tg(t) around tg(t) around tg(t) in the counterclockwise sense. For a given value of tg(t) of this function on tg(t) differs from that on tg(t)0 by tg(t)1. Hence the total integral is simply tg(t)2 times the integral (A 11) (the short vertical segments of tg(t)3 contour manipulation and the resulting factorization.

Noting that g(t) is a meromorphic function we are led to the identity

$$(\log L^{+})'(\xi) = \frac{1}{2\pi i} \sum_{C} \operatorname{res} \left\{ [\log L(-k_{\rm f} \cosh t)]' \frac{t \sinh t}{\cosh t - \cosh u} \right\}, \tag{A 12}$$

where the sum is over all simple poles within C.

(c) Evaluating the residues

There are two poles associated with ξ at t=u and $t=2\pi \mathrm{i}-u$. The value of ξ is the same at both, but $\gamma(s(2\pi \mathrm{i}-u))=-\gamma(s(u))$. Thus, the first pole is 'physical' in the sense that its value of γ satisfies the radiation conditions, while the second pole is 'unphysical'. In particular, $\log L(s(2\pi \mathrm{i}-u))=-\log L(s(u))$, from which it follows that

$$\frac{1}{2\pi i} \sum_{\xi - \text{poles}} \operatorname{res} \left\{ \frac{t \sinh t (\log L)'}{\cosh t - \cosh u} \right\} = \frac{2(u - i\pi)}{2\pi i} [\log L(\xi)]'$$

$$= -\frac{1}{\pi} [\log L(\xi)]' \cos^{-1}(\xi/k_{\text{f}}). \tag{A 13}$$

The appropriate branch for the inverse cosine is

$$\cos^{-1}(\xi/k_{\rm f}) = -i\log[\xi/k_{\rm f} - \gamma(\xi)/k_{\rm f}], \tag{A 14}$$

where $\log z = \log |z| + i\theta$, $-\pi < \theta < \pi$, which when combined with the identity $\cosh^{-1}(-z) = i\pi - i\cos^{-1}z$ ensures that the regions in the complex ξ -plane are mapped into the sectors of the t-plane as shown in figure 11.

We now consider the poles of $(\log L)' = (\log R_2)' - (\log R_1)'$, which can be simplified by using the definition (4.9):

$$[\log R(\xi)]' = \frac{\widetilde{D}'}{\widetilde{D}} - \frac{D'}{D}.$$
 (A 15)

The region inside C contains two replicas of both the 'physical' and the 'unphysical' transform planes, where $\operatorname{Re}_{\gamma}(\xi) \geqslant 0$ in the former and $\operatorname{Re}_{\gamma}(\xi) \leqslant 0$ in the latter. Thus, the poles of D and \widetilde{D} are the roots $\pm \xi_n$, $n=1,2,\ldots,\frac{1}{2}N$, of the polynomial P of $(A\ 3)$. Recall that $\operatorname{Im}_{\xi_n} > 0$, with $\xi_n = -k_f \cosh t_n$, where t_n lie in the 'upper physical' and 'upper unphysical' quadrants of C. Those in the former quadrant correspond to roots of the dispersion relation $D(\xi) = 0$ and the others solve $\widetilde{D}(\xi) = 0$. In any event, it is important to realize that all the roots of P = 0 are involved in the residue evaluation for both terms in $(A\ 15)$. In addition to the poles at $t = t_n$ there are poles at $t = 3\pi \mathbf{i} - t_n$, corresponding to the roots $-\xi_n$. Note that the value of $\gamma(s(t)) = -k_f \sinh t$ is the same at $t = t_n$ and $t = 3\pi \mathbf{i} - t_n$. The residues at these poles are simple to calculate, taking into account the fact that $dD(s)/dt = -k_f \sinh t D'(s)$. Let $\frac{1}{2}\tilde{N} \leqslant \frac{1}{2}N$ be the number of zeros of \tilde{D} , arranged such that the first $\frac{1}{2}(N-\tilde{N})$ roots ξ_n are the zeros of D. It follows from these considerations that the first $\frac{1}{2}(N-\tilde{N})$ poles give

$$-\frac{1}{2\pi i} \sum_{n=1}^{(N-\tilde{N})/2} \operatorname{res} \left\{ \frac{t \sinh t}{\cosh t - \cosh u} \left(\frac{D'}{D} - \frac{\tilde{D}'}{\tilde{D}} \right) \right\} \Big|_{\xi_n}$$

$$= \frac{1}{2\pi i k_{\rm f}} \sum_{n=1}^{(N-\tilde{N})/2} \left\{ \frac{t_n}{\cosh t_n - \cosh u} - \frac{(2\pi i - t_n)}{\cosh t_n - \cosh u} - \frac{(3\pi i - t_n)}{\cosh t_n + \cosh u} + \frac{(\pi i + t_n)}{\cosh t_n + \cosh u} \right\}$$

$$= \frac{1}{\pi i} \sum_{n=1}^{(N-\tilde{N})/2} \frac{2\xi_n (i\pi - t_n)}{\xi_n^2 - \xi^2}. \tag{A 16}$$

The four terms in (A 16) arise from, in succession, the pole of D at ξ_n (t_n) in the upper physical sector; the pole of \widetilde{D} at ξ_n ($2\pi \mathbf{i} - t_n$) in the upper unphysical sector; the pole of D at $-\xi_n$ ($3\pi \mathbf{i} - t_n$) in the lower physical sector; and the pole of \widetilde{D} at $-\xi_n$ ($\pi \mathbf{i} + t_n$) in the upper unphysical sector. A similar result follows for the remaining \widetilde{N} roots, i.e.

$$-\frac{1}{2\pi i} \sum_{n=((N-\tilde{N})/2)+1}^{N/2} \operatorname{res} \left\{ \frac{t \sinh t}{\cosh t - \cosh u} \left(\frac{D'}{D} - \frac{\tilde{D}'}{\tilde{D}} \right) \right\} \Big|_{\xi_n}$$

$$= -\frac{1}{\pi i} \sum_{n=((N-\tilde{N})/2)+1}^{N/2} \frac{2\xi_n (i\pi - t_n)}{\xi_n^2 - \xi^2}. \quad (A 17)$$

Equations (A 16) and (A 17) may be combined, by using (A 15), to give

$$\frac{1}{2\pi i} \sum_{\xi_n - \text{poles}} \text{res} \left\{ \frac{t \sinh t (\log R)'}{\cosh t - \cosh u} \right\} = \frac{1}{\pi} \sum_{n=1}^{N} \frac{2\xi_n \theta_n s_n}{\xi_n^2 - \xi^2}, \tag{A 18}$$

where

$$s_n = \begin{cases} 1, & \text{for physical roots,} \\ -1, & \text{for unphysical roots.} \end{cases}$$
 (A 19)

Recall that the two membrane roots are unphysical. Also, the angle $\theta_n = \pi + it_n$, or specifically,

$$\theta_n = \cos^{-1}(\xi_n/k_f),\tag{A 20}$$

where the branch of the inverse cosine is given by (A 14).

(d) Number of physical roots

By applying the principle of the argument to the dispersion function (4.3), the number of physical roots with $\operatorname{Re} \gamma(\xi) \geqslant 0$ can be determined. Recall that this principle states that if a function $f(\xi)$ is analytic on a simple closed curve C, except for a finite number of poles within C and no zeros on C, then

$$\frac{1}{2\pi i} \int_C \frac{\mathrm{d}f}{\mathrm{d}\xi} \frac{\mathrm{d}\xi}{f(\xi)} = n_z - n_p, \tag{A21}$$

where n_z, n_p are the number of zeros and poles in C, respectively.

Here we consider the dispersion relation $D(\xi) = 0$ given by (4.3) which has no poles $(n_p = 0)$ so that (A 21) will then count the number of zeros. First, we rewrite the dispersion function in terms of γ giving $D(\xi) = \mathcal{D}(\gamma)$, and by using (A 21) to get

$$n_{\mathbf{z}} = \int_{C'} \mathbf{d}[\log \mathcal{D}(\gamma)].$$
 (A 22)

By counting the number of times the contour C' encircles the origin in the counter-clockwise direction as γ is varied along the contour enclosing the half-space $\text{Re}\,\gamma>0$, the number of physical roots is determined. For the situation considered here, a curved plate, it was found that there are always three physical roots, and therefore four unphysical ones because there are seven in total. The three physical roots are similar to those obtained for a flat plate which has three physical and two unphysical roots. By curving the plate, coupling between flexural and longitudinal motion occurs but the two longitudinal roots are always unphysical.

(e) Various forms of K^+

Combining (A12), (A13) and (A18), we have

$$L^{+}(\xi) = \left[\frac{R_1(0)}{R_2(0)}\right]^{1/2} e^{\left[\Phi_1(\xi) - \Phi_2(\xi)\right]},\tag{A 23}$$

where

$$\Phi(\xi) = \frac{1}{\pi} \int_0^{\xi} \left[\sum_{n=1}^{N/2} \frac{2\xi_n \theta_n s_n}{s^2 - \xi_n^2} + [\log R(s)]' \cos^{-1}(s/k_f) \right] ds, \tag{A 24}$$

and the value at $\xi = 0$ follows from the definition and symmetry of L^{\pm} . Equations (A 9) and (A 23) now imply that

$$K^{+}(\xi) = \left[\frac{P_{2}^{+}(\xi)}{P_{1}^{+}(\xi)}\right]^{1/2} \left[\frac{R_{1}(0)}{R_{2}(0)}\right]^{1/4} e^{\left[\Phi_{1}(\xi) - \Phi_{2}(\xi)\right]/2}, \tag{A 25}$$

and it is clear that this automatically satisfies the condition (A 2). This can be seen by using (A 4)-(A 7). The main effort in calculating the split function for finite values

of the argument is thus reduced to evaluating the integral $(\Phi_1 - \Phi_2)$. Equation (A 25) expresses K^+ in a form which is easily evaluated for small values of ξ . We note that the integrand possesses no poles in the upper half-plane, \mathcal{H}^+ , because the poles of R are exactly cancelled by the poles in the first term in the integrand.

This can be observed by expressing the second term of (A 24) in partial fractions. Note that $(\log R)'(\xi)$ can be written as

$$(\log R)'(\xi) = R'(\xi)/R(\xi) = 1/\gamma(\xi)Q(\xi),$$
 (A 26)

where $Q(\xi)$ is the ratio of two polynomials and is given by

$$Q = P/(\tilde{D}'D - \tilde{D}D')\gamma. \tag{A 27}$$

Since only P appears in the numerator of Q, they share the same zeros and

$$\operatorname{res}[1/Q(\xi)]|_{\xi=\pm\xi_n} = -s_n \gamma(\xi_n). \tag{A 28}$$

Thus,

$$(\log R)'(\xi) = \sum_{n=1}^{N/2} \frac{-2\xi s_n}{\xi^2 - \xi_n^2} \frac{\gamma(\xi_n)}{\gamma(\xi)}.$$
 (A 29)

Substituting (A 29) into (A 24) and using (A 20), we then obtain

$$\Phi(\xi) = \frac{2}{\pi} \int_{\pi/2}^{\cos^{-1} \xi/k_{\rm f}} \sum_{n=1}^{N/2} \frac{\theta \cos \theta \sin \theta_n - \theta_n \cos \theta_n \sin \theta}{\cos^2 \theta - \cos^2 \theta_n} s_n \, \mathrm{d}\theta. \tag{A 30}$$

An alternative form for K^+ can be found by factorizing the denominator of (A 30) and using (A 7) to obtain

$$K^{+}(\xi) = \left[\frac{D_2(0)}{D_1(0)}\right]^{1/2} \prod' \frac{1 + \xi/\xi_n^{(2)}}{1 + \xi/\xi_n^{(1)}} e^{[\phi_1(\xi) - \phi_2(\xi)]}, \tag{A 31}$$

where the products \prod' are taken over the roots for which $s_n = 1$, and

$$\phi(\xi) = \frac{1}{2\pi} \int_{\pi/2}^{\cos^{-1} \xi/k_{\rm f}} \sum_{n=1}^{N/2} \left[\frac{\theta \sin \theta_n - \theta_n \sin \theta}{\cos \theta - \cos \theta_n} + \frac{\theta \sin \theta_n - (\pi - \theta_n) \sin \theta}{\cos \theta + \cos \theta_n} \right] s_n \, \mathrm{d}\theta.$$
(A 32)

Evidently, $\phi_1 - \phi_2 \to 0$ in the limit of light fluid loading. This form of K^+ is preferred for numerical computations because it does not contain any square roots in the pre-exponent.

The main attraction of the Wiener-Hopf split function K^+ as given by either (A 25) or (A 31) is the finite interval of integration in equations (A 30) and (A 32), which permits fast numerical evaluation. Abrahams & Lawrie (1995) describe a fundamentally different finite-integral factorization procedure based upon Malyuzhinets functions.

Appendix B. Expansion coefficients

(a) Asymptotic forms for K^+

Equations (4.3), (4.4), (5.12) and (A1) imply that the value of $K^+(\xi)$ at infinity, denoted by K_{∞}^+ , is

$$K_{\infty}^{+} = \lim_{\xi \to \infty} \left[\frac{P_2^{+}(\xi)}{P_1^{+}(\xi)} \right]^{1/2} = \sqrt{\mu},$$
 (B1)

where $\mu = B_2/B_1$. It is then easily seen from (A 25) that

$$K^{+}(\xi) = \left[\frac{P_2^{+}(\xi)}{P_1^{+}(\xi)}\right]^{1/2} \exp[\Phi_2^{\infty}(\xi) - \Phi_1^{\infty}(\xi)], \tag{B2}$$

where

$$\Phi^{\infty} = \frac{1}{2\pi} \int_{\xi}^{\infty} \left[\sum_{n=1}^{N/2} \frac{2\xi_n \theta_n}{s^2 - \xi_n^2} + [\log R(s)]' \cos^{-1}(s/k_f) \right] ds.$$
 (B 3)

The latter expression has the virtue that it is easy to expand about the point at infinity in the complex ξ -plane once we have determined that the appropriate branch of the inverse cosine is

$$i\cos^{-1}(\xi/k_{\rm f}) = \log(2\xi/k_{\rm f}) - k_{\rm f}^2/(4\xi^2) + O(\xi^{-4}).$$
 (B4)

Further, a routine calculation yields

$$\frac{\mathrm{d}}{\mathrm{d}\xi}[\log R(\xi)] = -\frac{10\kappa^4}{a\xi^6} - \frac{7k_{\rm f}^2\kappa^4}{a\xi^8} + O(\xi^{-10}),\tag{B5}$$

and so expanding the integrand in (B3) and then integrating term by term we find that

$$\frac{K^{+}(\xi)}{K_{\infty}^{+}} = \exp\left[\sum_{n=1}^{5} \frac{1}{\xi^{n}} (\beta_{n}^{(2)} - \beta_{n}^{(1)}) - \frac{\mathrm{i}}{\pi \xi^{5}} \left(\frac{\kappa_{2}^{4}}{a_{2}} - \frac{\kappa_{1}^{4}}{a_{1}}\right) \log\left(\frac{2\xi}{k_{\mathrm{f}}}\right) + O(\xi^{-6})\right], \quad (B6)$$

where, for the sake of convenience, we have promoted the prefactor in (B 3) into the exponent before expanding. The coefficients are all explicitly expressed in terms of the zeros of $P_1(\xi)$ and $P_2(\xi)$ as

$$\beta_j^{(k)} = \frac{1}{2j} \sum_{n=1}^{7} \left\{ \frac{\theta_n^{(k)}}{\pi} \left[(\xi_n^{(k)})^j - (-\xi_n^{(k)})^j \right] - (-\xi_n^{(k)})^j \right\}.$$
 (B7)

The expansions of the functions \tilde{p}_0^{\pm} and \tilde{w}_0^{\pm} for large ξ are straightforward except for the terms involving $K^{\pm}(\xi)$ (see equation (6.7)). Combining all terms in the exponent, we have from equations (B 6) and (6.6) that

$$\frac{K^{\pm}(\xi)}{(\xi - \xi_0)P^*(\xi)} = \frac{K_{\infty}^{\pm}}{P_0^*} \xi^{-(1+N^*)} \exp\left[\sum_{n=1}^4 \frac{\beta_n^{\pm}}{\xi^n} + O(\xi^{-5}\log\xi)\right]
= \frac{K_{\infty}^{\pm}}{P_0^*} \sum_{n=0}^4 \frac{\delta_n^{\pm}}{\xi^{(1+N^*+n)}} + O(\xi^{-14}\log\xi),$$
(B8)

where $K_{\infty}^{-} = 1/K_{\infty}^{+}$, P_{0}^{*} is defined in (6.5),

$$\beta_j^{\pm} = (\pm 1)^{j-1} (\beta_j^{(2)} - \beta_j^{(1)}) + \frac{1}{j} \left\{ (\xi_0)^j + \sum_{n=1}^{N^*/2} [(\zeta_n)^j + (-\zeta_n)^j] \right\}$$
 (B9)

and

$$\delta_0^{\pm} = 1,$$
 (B 10 a)

$$\delta_1^{\pm} = \beta_1^{\pm},$$
 (B 10 b)

$$\delta_2^{\pm} = \frac{1}{2} (\beta_1^{\pm})^2 + \beta_2^{\pm}, \tag{B 10 c}$$

$$\delta_3^{\pm} = \frac{1}{6} (\beta_1^{\pm})^3 + \beta_1^{\pm} \beta_2^{\pm} + \beta_3^{\pm}, \tag{B 10 d}$$

$$\delta_4^{\pm} = \frac{1}{24} (\beta_1^{\pm})^4 + \frac{1}{2} (\beta_1^{\pm})^2 \beta_2^{\pm} + \frac{1}{2} (\beta_2^{\pm})^2 + \beta_1^{\pm} \beta_3^{\pm} + \beta_4^{\pm}.$$
 (B 10 e)

(b) Expansions for
$$\tilde{w}_0^{\pm}$$
 and \tilde{p}_0^{\pm}

The expansion for \tilde{w}_0^{\pm} of equation (6.7), and of \tilde{p}_0^{\pm} , imply by using (6.11), (6.12) and (6.15) that

$$\lambda_n^{\pm} = G(\xi_0) \left\{ \frac{U_1(\xi_0) K^+(\xi_0)}{P^*(\xi_0)} (\xi_0)^n + \sum_{m=1}^{N^*/2} \left[\frac{u_{1m}^+(\zeta_m)^n}{\zeta_m - \xi_0} - \frac{u_{2m}^-(-\zeta_m)^n}{\zeta_m + \xi_0} \right] - \frac{K_{\infty}^{\pm}}{P_0^*} \sum_{l=0}^2 \delta_{n+l-N^*}^{\mp} U_l^{\pm} \right\}, \quad n = 0, \dots, 10, \quad (B \, 11 \, a)$$

$$\psi_n^{\pm} = G(\xi_0) \left\{ -\frac{V_1(\xi_0)K^+(\xi_0)}{P^*(\xi_0)} (\xi_0)^n - \sum_{m=1}^{N^*/2} \left[\frac{v_{1m}^+(\zeta_m)^n}{\zeta_m - \xi_0} - \frac{v_{2m}^-(-\zeta_m)^n}{\zeta_m + \xi_0} \right] + \frac{K_{\infty}^{\mp}}{P_0^*} \sum_{l=2}^{6} \delta_{n+l-N^*}^{\mp} V_l^{\pm} \right\}, \quad n = 0, \dots, 6, \quad (B \, 11 \, b)$$

where V_j^-, V_j^+, U_j^- and U_j^+ are the coefficients of ξ^j in $V_1(\xi), V_2(\xi), U_1(\xi)$ and $U_2(\xi)$, respectively. Thus, for example, $V_2^- = a_1, V_4^- = k_1^2 a_1/\kappa_1^4, V_6^- = -a_1/\kappa_1^4$, while $U_0^- = k_1^2$ and $U_2^- = -1$. Also, $\delta_n^\pm = 0$ for n < 0 and n > 4 in (B 11), and (cf. (6.8))

$$v_{jn}^{\pm} = \text{residue of } \left[\frac{V_j(\xi)K^{\pm}(\xi)}{P^*(\xi)} \right]_{\xi = \pm \zeta_n}.$$
 (B 12)

We note that $v_{2n}^- = -v_{1n}^+/K^-K^+$, which may be used in conjunction with the analogous result (6.10) to simplify equation (B 11).

The λ and ψ may be easily computed by using the following recursion relations:

$$\tilde{\lambda}_{n}^{\pm} = \lambda_{n+1}^{\pm} - \xi_{0} \lambda_{n}^{\pm}$$

$$= G(\xi_{0}) \sum_{m=1}^{4} [(\zeta_{m})^{n} u_{1m}^{+} + (-\zeta_{m})^{n} u_{2m}^{-}]$$

$$- \frac{K_{\infty}^{\mp}}{P_{0}^{*}} G(\xi_{0}) \sum_{l=0}^{2} (\delta_{n+l-7}^{\mp} - \xi_{0} \delta_{n+l-8}^{\mp}) U_{l}^{\pm}, \quad n = 0, \dots, 9, \qquad (B 13 a)$$

$$\tilde{\psi}_{n}^{\pm} = \psi_{n+1}^{\pm} - \xi_{0} \psi_{n}^{\pm}$$

$$= -G(\xi_{0}) \sum_{m=1}^{4} [(\zeta_{m})^{n} v_{1m}^{+} + (-\zeta_{m})^{n} v_{2m}^{-}]$$

$$+ \frac{K_{\infty}^{\mp}}{P_{0}^{*}} G(\xi_{0}) \sum_{l=2}^{6} (\delta_{n+l-7}^{\mp} - \xi_{0} \delta_{n+l-8}^{\mp}) V_{l}^{\pm}, \quad n = 0, \dots, 5. \qquad (B 13 b)$$

Finally, we note that for acoustic or shell wave incidence (i.e. when $A_0 \neq 0$) the first terms in (B 11 a) and (B 11 b) can be simplified by using

$$G(\xi_0)U_1(\xi_0)\frac{K^+(\xi_0)}{P^*(\xi_0)} = \frac{1}{A_0}p_{,y}^{(0)}(0,0),$$
(B 14 a)

$$-G(\xi_0)V_1(\xi_0)\frac{K^+(\xi_0)}{P^*(\xi_0)} = \frac{1}{A_0}p^{(0)}(0,0).$$
 (B 14 b)

Appendix C. Meaning for the roots of $P^*(\xi) = 0$

Consider a sandwich composed of plates 1 and 2 with a fluid layer of thickness 2d between them and a vacuum above and below. The sandwich is considered as flat, with the equations of motion for each plate governed by the operator \mathcal{L}_j , j=1 or 2. To be specific, let plate 1 lie above plate 2, and they are situated at y=d and y=-d, respectively. Define w_1 (w_2) as the downward (upward) displacement of plate 1 (2). The equations of motion are then

$$V_1\left(-i\frac{\mathrm{d}}{\mathrm{d}x}\right)\rho_f\omega^2w_1(x) = -U_1\left(-i\frac{\partial}{\partial x}\right)p(x,d),\tag{C1} a)$$

$$V_2\left(-i\frac{\mathrm{d}}{\mathrm{d}x}\right)\rho_f\omega^2w_2(x) = -U_2\left(-i\frac{\partial}{\partial x}\right)p(x,-d),\tag{C1b}$$

where p is the pressure in the fluid layer. Consider a breathing type of motion of the sandwich, for which

$$w_1(x) = w(x), \quad w_2(x) = w(x)/\Gamma,$$
 (C2)

and p satisfies

$$p(x,d) - \Gamma p(x,-d) = 0. \tag{C3}$$

Then it follows that w satisfies the equation of motion

$$P^* \left(-i \frac{\mathrm{d}}{\mathrm{d}x} \right) \rho_{\mathrm{f}} \omega^2 w(x) = U_1 \left(-i \frac{\partial}{\partial x} \right) U_2 \left(-i \frac{\partial}{\partial x} \right) (p(x, d) - \Gamma p(x, -d))$$

$$= 0, \tag{C4}$$

where P^* is the polynomial defined in equation (6.5). A solution of the form,

$$\rho_{\rm f}\omega^2 w(x) = e^{i\zeta_n x},\tag{C5}$$

automatically satisfies (C4), and the associated pressure is

$$p(x,y) = [p_{s}\cos(\gamma(\zeta_{n})y) + p_{a}\sin(\gamma(\zeta_{n})y)]e^{i\zeta_{n}x}.$$
 (C6)

Equations (C1) and (C3) imply that

$$p_{\rm s} = \left(\frac{\Gamma + 1}{2\Gamma}\right) \frac{\sec(\gamma(\zeta_n)d)}{\gamma(\zeta_n)X} p_{\rm a} = \left(\frac{\Gamma - 1}{2\Gamma}\right) \frac{\csc(\gamma(\zeta_n)d)}{\gamma(\zeta_n)X},\tag{C7}$$

where

$$X = -\frac{U_1(\zeta_n)}{V_1(\zeta_n)\gamma(\zeta_n)} = -\frac{U_2(\zeta_n)}{V_2(\zeta_n)\gamma(\zeta_n)}.$$
 (C8)

The continuity condition at the two plates, (2.3), is then satisfied if and only if both

$$\Gamma = 1$$
 and $\tan(\gamma(\zeta_n)d) = X.$ (C9)

Therefore, a root ζ_n of $P^*(\zeta_n) = 0$ which satisfies the identity $(C 9)_2$ corresponds to a symmetric free wave of the sandwich. The mode shape is such that $w_1 = w_2$ and p is symmetric about the centre.

Appendix D. Two membranes

The structural dynamics are governed by the equations

$$-T_j w_{,xx} - m_j \omega^2 w = -p, \quad j = 1, \quad x < 0; \quad j = 2, \quad x > 0,$$
 (D1)

where the 'tensions' $T_{1,2} > 0$ will be allowed to differ. The general theory can now be applied, with

$$U_j = 1, \quad V_j = a_j(\xi^2/\bar{k}_j^2 - 1),$$
 (D2)

where $\bar{k}_{1,2}^2 \equiv m_j \omega^2 / T_j$ are the membrane wave numbers, and $a_{1,2}$ are defined by $(2.5)_3$. The reflection coefficient polynomial P^* is quadratic $(N^* = 2)$ with

$$P_0^* = \frac{a_1}{\bar{k}_1^2} - \frac{a_2}{\bar{k}_2^2}, \quad \zeta_1^2 = \frac{a_1 - a_2}{P_0^*} = \bar{k}_1^2 \left(\frac{\alpha - 1}{\bar{\mu} - 1}\right),$$
 (D 3)

where α is given by $(6.26)_1$, and $\bar{\mu} = T_2/T_1$ is the stiffness ratio, analogous to μ of equation (6.24) for the plate.

There are two junction conditions for the continuity of w and $Tw_{,x}$, implying q=2. The first condition is exactly the same as $(6.23\,a)$, and the second is similar to $(6.23\,c)$:

$$\bar{\mu}\Lambda_1^+ - \Lambda_1^- = \xi_0(\bar{\mu} - 1)p_y^{(0)}(0, 0).$$
 (D4)

In this particular problem $\lambda_j^+ = \lambda_j^-$ for j = 0 and j = 1, only, but this implies, by using (6.23 a), that $\bar{A}_2 = 0$. The remaining two equations, (6.17) and (D 4), become

$$\begin{bmatrix} 1 & \xi_0 \\ (\bar{\mu} - 1)\lambda_1^{\pm} & \bar{\mu}\lambda_2^{+} - \lambda_2^{-} \end{bmatrix} \begin{bmatrix} \bar{A}_0 \\ \bar{A}_1 \end{bmatrix} = \begin{bmatrix} A_0 \\ \xi_0(\bar{\mu} - 1)p_{,y}^{(0)}(0,0) \end{bmatrix}.$$
 (D 5)

Redefine A according to

$$A(\xi) = A_0 + (\xi - \xi_0)\tilde{A}_1, \tag{D6}$$

then (D5) implies that

$$\tilde{A}_1 = (\bar{\mu} - 1) \left[\frac{\xi_0 p_{,y}^{(0)}(0,0) - \lambda_1^{\pm} A_0}{\bar{\mu}(\lambda_2^+ - \xi_0 \lambda_1^{\pm}) - (\lambda_2^- - \xi_0 \lambda_1^{\pm})} \right]. \tag{D7}$$

The denominator can be reduced by using

$$\lambda_{2}^{\pm} - \xi_{0}\lambda_{1}^{\pm} = G(\xi_{0})[\zeta_{1}(u_{11}^{+} - u_{21}^{-}) - (\bar{\mu})^{\mp 1/2}/P_{0}^{*}]$$

$$= \frac{G(\xi_{0})}{P_{0}^{*}}(\cosh \nu_{1} - (\bar{\mu})^{\mp 1/2}), \tag{D8}$$

which follows from (6.10), (B 11) with $K_{\infty}^+ = \sqrt{\mu}$, the fact that $K^-(\zeta_1) = K^+(\zeta_1)$ because $K(\zeta_1) = 1$, and the definition

$$\nu_1 = \log K^+(\zeta_1). \tag{D9}$$

The numerator in (D7) simplifies by using the identity (B14), yielding

$$\tilde{A}_1 = -A_0(\xi_0 + \zeta_1 \tanh \nu_1) / (\zeta_1^2 - \xi_0^2). \tag{D 10}$$

Finally, we obtain the polynomial

$$A(\xi) = \frac{A_0}{\zeta_1^2 - \xi_0^2} [\zeta_1^2 - \xi \xi_0 - (\xi - \xi_0) \zeta_1 \tanh \nu_1].$$
 (D 11)

It is easily verified that this satisfies the reciprocity condition (5.29). Also note that the pressure is continuous at the origin, p(+0,0) = p(-0,0), because $\psi_j^+ = \psi_j^-$ for j=0 and j=1.

(a) Light fluid-loading limit

The limit of light fluid loading is defined here as the limit in which the lengths $a_{1,2}$ far exceed all other lengths in the problem. Consequently, the function K can be approximated as $K = V_1/V_2$, with the explicit split functions

$$K^{+}(\xi) = \sqrt{\mu} \left(\frac{\bar{k}_2 + \xi}{\bar{k}_1 + \xi} \right), K^{-}(\xi) = \frac{1}{\sqrt{\mu}} \left(\frac{\bar{k}_1 - \xi}{\bar{k}_2 - \xi} \right), \tag{D 12}$$

and the generalized dispersion function of (5.16) becomes

$$G(\xi) = -\gamma \frac{\sqrt{a_1 a_2}}{\bar{k}_1 \bar{k}_2} (\xi + \bar{k}_1)(\xi - \bar{k}_2). \tag{D 13}$$

The transform of the scattered pressure, from (5.15), is

$$\tilde{p}(\xi) = \frac{iA(\xi)}{\xi - \xi_0} \frac{(\xi_0 + \bar{k}_1)(\xi_0 - \bar{k}_2)}{(\xi + \bar{k}_1)(\xi - \bar{k}_2)}.$$
(D 14)

Equations (D 3), (D 12) yield, after some algebra,

$$\zeta_1 \tanh \nu_1 = \bar{k}_1 \left(\frac{\alpha - 1}{1 + \sqrt{\alpha \bar{\mu}}} \right),$$
(D 15)

which, combined with (D 11), gives an explicit expression for A.

Consider a membrane wave incident from the left, for which $\xi_0 \approx \bar{k}_1$ and $A_0 = 1$. The reflection coefficient for the membrane wave travelling back to the left is then $R_{\text{mem}} = (-i) \operatorname{res} \tilde{p}(-\bar{k}_1)$, which can be evaluated by using equations (D 11), (D 15) and (D 14), giving

$$R_{\text{mem}} = \frac{\sqrt{\alpha \bar{\mu}} - 1}{\sqrt{\alpha \bar{\mu}} + 1}.$$
 (D 16)

This agrees with the expected result, $R_{\rm mem}=(Z_2-Z_1)/(Z_2+Z_1)$, where $Z_j=m_jc_j$ is the membrane wave impedance for membrane $j,\ j=1,2$ and $c_j=\omega/\bar{k}_j$ are the membrane wave speeds. The equivalence follows from the identity $\sqrt{\alpha\bar{\mu}}=Z_2/Z_1$, and is expected because membrane wave reflection and transmission is only weakly affected under light fluid loading.

As a second example, consider an incident acoustic wave, with A_0 given by equation (5.7). The diffracted acoustic wave depends upon the diffraction coefficient of equation (5.22), which becomes, by using (4.12) and the above equations,

$$C(\theta, \theta_0) = \left(\frac{\bar{k}_2^2}{a_2} - \frac{\bar{k}_1^2}{a_1}\right) \frac{\gamma(\xi)}{\gamma(\xi_0)} \frac{\left[\zeta_1^2 - \xi \xi_0 - (\xi - \xi_0)\zeta_1 \tanh \nu_1\right]}{(\xi - \xi_0)(\xi + \bar{k}_1)(\xi - \bar{k}_2)(\xi_0 - \bar{k}_1)(\xi_0 + \bar{k}_2)}.$$
 (D 17)

This is small, of order 1/a, as expected. It is also real-valued, and possesses singularities corresponding to the specular direction ($\xi = \xi_0$), forced incident membrane waves ($\xi_0 = \bar{k}_1, -\bar{k}_2$) and forced 'radiating' membrane waves ($\xi = -\bar{k}_1, \bar{k}_2$). These singularities appear because we are implicitly neglecting the acoustic feedback between the membrane and the fluid in the light fluid limit. The membrane waves are either subsonic or leaky in the full solution, and are therefore not excitable by an incident acoustic plane wave. Their appearance in (D 17) indicates that the light fluid-loading approximation becomes invalid for incident wave number in the vicinity of one of these wave numbers, and a different ansatz is required. Thus, the ξ_0 poles correspond to the fact that the 'incidence' or forcing is dominated by a membrane wave, not just an acoustic wave, and the ξ poles can be viewed similarly in terms of reciprocity.

(b) Heavy fluid-loading approximation

The converse physical limit in which $a_{1,2}$ are much shorter than all other physical lengths is called the heavy fluid-loading limit. The acoustic reflection coefficients $R_{1,2}$ are approximately -1 in this case, as compared with +1 in the light fluid-loading regime. In fact the leading-order approximation is now much simpler, because $K(\xi) \approx 1$, implying $K^{\pm}(\xi) \approx 1$ and $G(\xi) \approx 1$. Thus, (D 11) reduces to

$$A(\xi) = A_0 \frac{\zeta_1^2 - \xi \xi_0}{\zeta_1^2 - \xi_0^2}.$$
 (D 18)

Furthermore, the scattered acoustic response is simply $\tilde{p} \approx iA(\xi)/(\xi - \xi_0)$. For example, the acoustic diffraction coefficient becomes

$$C(\theta, \theta_0) \approx \frac{\gamma(\xi)\gamma(\xi_0)}{\xi_0 - \xi} \left[\left(\frac{a_1}{\bar{k}_1^2} - \frac{a_2}{\bar{k}_2^2} \right) \xi \xi_0 - (a_1 - a_2) \right],$$
 (D 19)

which is again real and small.

References

- Abrahams, I. D. & Lawrie, J. B. 1995 On the factorization of a class of Wiener-Hopf kernels. IMA J. Appl. Math. 55, 35–47.
- Brazier-Smith, P. R. 1987 The acoustic properties of two coplanar half-plane plates. *Proc. R. Soc. Lond.* A **409**, 115–139.
- Cannell, P. A. 1975 Edge scattering of aerodynamic sound by a lightly loaded elastic half-plane. Proc. R. Soc. Lond. A 347, 213–238.
- Cannell, P. A. 1976 Acoustic edge scattering by a heavily loaded elastic half-plane. Proc. R. Soc. Lond. A 350, 71–89.
- Clemmow, P. C. 1953 Radio propagation over a flat Earth across a boundary separating two different media. *Phil. Trans. R. Soc. Lond.* A **246**, 1–55.
- Crighton, D. G. 1971 Acoustic beaming and reflexion from wave-bearing surfaces. *J. Fluid Mech.* 47, 625–638.
- Crighton, D. G. 1972 Force and moment admittance of plates under arbitrary fluid loading. *J. Sound Vib.* **20**, 209–218.
- Crighton, D. G. 1979 The free and forced waves on a fluid-loaded elastic plate. *J. Sound Vib.* **63**, 225–235.
- Crighton, D. G., Dowling, A. P., Ffowcs Williams, J. E., Heckl, M. & Leppington, F. G. 1992 *Modern methods in analytical acoustics: lecture notes.* New York: Springer.
- Crighton, D. G. & Innes, D. 1984 The modes, resonances and forced response of elastic structures under heavy fluid loading. *Phil. Trans. R. Soc. Lond.* A 312, 295–341.
- Crighton, D. G. & Leppington, F. G. 1970 Scattering of aerodynamic noise by a semi-infinite compliant plate. *J. Fluid Mech.* 43, 721–736.
- Heins, A. E. & Feshbach, H. 1954 On the coupling of two half planes. *Proc. Symp. Appl. Math* 5, 75–87.
- Kay, A. F. 1959 Scattering of a surface wave by a discontinuity in reactance. IRE Trans. Antennas Propag. AP-7, 22–31.
- Mace, B. R. 1984 Wave reflection and transmission in beams. J. Sound Vib. 97, 237-246.
- Noble, B. 1958 Methods based on the Wiener-Hopf technique. New York: Pergamon.
- Norris, A. N. & Rebinsky, D. A. 1994 Acoustic coupling to membrane waves on elastic shells. J. Acoust. Soc. Am. 95, 1809–1829.

- Norris, A. N. & Rebinsky, D. A. 1995 Acoustic and membrane wave interaction at plate junctions. J. Acoust. Soc. Am. 97, 2063–2073.
- Norris, A. N. & Wickham, G. R. 1995 Acoustic diffraction from the junction of two flat plates. *Proc. R. Soc. Lond.* A **451**, 631–655.
- Photiadis, D. M. 1995 Transport of energy across a discontinuity by fluid loading. *J. Acoust. Soc. Am.* **97** 1409–1414.
- Pierce, A. D. 1993 Variational formulations in acoustic radiation and scattering. In *Physical acoustics* (ed. A. D. Pierce & R. N. Thurston), vol. 22, pp. 195–371. New York: Academic.
- Rebinsky, D. A. & Harris, J. G. 1992 An asymptotic calculation of the acoustic signature of a cracked surface for the line focus scanning acoustic microscope. *Proc. R. Soc. Lond.* A **436**, 251–265.
- Rebinsky, D. A. & Norris, A. N. 1995a Longitudinal and shear wave diffraction at the junction of two fluid loaded, doubly curved shells. *Wave Motion* 22, 31–46.
- Rebinsky, D. A. & Norris, A. N. 1995b Acoustic and flexural wave scattering from a three member junction. J. Acoust. Soc. Am. 98, 3309–3319.
- Senior, T. B. A. 1952 Diffraction by a semi-infinite metallic sheet. Proc. R. Soc. Lond. A 213, 436–458.
- Wickham, G. R. 1995 Mode conversion, corner singularities and matrix Wiener-Hopf factorization in diffraction theory. Proc. R. Soc. Lond. A 451, 399–423.
- Wu, S. F. & Zhu, J. 1995a Sound radiation from two semi-infinite dissimilar plates subject to a harmonic line force excitation in mean flow. I. Theory. J. Acoust. Soc. Am. 97, 2709–2723.
- Wu, S. F. & Zhu, J. 1995b Sound radiation from two semi-infinite dissimilar plates subject to a harmonic line force excitation in mean flow. II. Asymptotics and numerical results. J. Acoust. Soc. Am. 97, 2709–2723.

		·	
1		I	
•		1	